safety

MDPI

Article

Risk Intensity and Exposure-Weighted Burden of Multiple Hazards in Serbia: A Nationwide Secondary Analysis of Public Health Emergency Assessments

Vladimir M. Cvetković [1,2,3,4,5,*], Dejan Ivanović [6], Velibor Lalić [7], Luka Sabljić [8], Jasmina Bašić [9], Vanja D. Cvetković [3] and Tin Lukić [10,11]

1 Department of Disaster Management and Environmental Security, Faculty of Security Studies, University of Belgrade, Gospodara Vučića 50, 11040 Belgrade, Serbia
2 Safety and Disaster Studies, Chair of Thermal Processing Technology, Department of Environmental and Energy Process Engineering, Technical University of Leoben, Franz Josef-Straße 18, 8700 Leoben, Austria
3 Scientific-Professional Society for Disaster Risk Management, Dimitrija Tucovića 121, 11040 Belgrade, Serbia; vanja.cvetkovic@spsdrm.org
4 International Institute for Disaster Research, Dimitrija Tucovića 121, 11040 Belgrade, Serbia
5 ProSafeNet—The Global Hub for Safety, Security, Risk, Emergency Professionals, and Scientists, 11040 Belgrade, Serbia
6 Institute of Public Health of Serbia "Dr Milan Jovanović Batut", Dr Subotića Starijeg 5, 11000 Belgrade, Serbia; dejan_ivanovic@batut.org.rs
7 Faculty of Security Science, University of Banja Luka, Bulevar Vojvode Živojina Mišića 10A, 78000 Banja Luka, Bosnia and Herzegovina; velibor.lalic@fbn.unibl.org
8 Faculty of Natural Sciences and Mathematics, University of Banja Luka, Mladena Stojanovića 2, 78000 Banja Luka, Bosnia and Herzegovina; luka.sabljic@pmf.unibl.org
9 College of Health Sciences, Academy of Applied Studies in Belgrade, Cara Dušana 254, 11080 Belgrade, Serbia; jasmina.basic@assb.edu.rs
10 Department of Geography, Tourism and Hotel Management, Faculty of Sciences, University of Novi Sad, Trg Dositeja Obradovića 3, 21000 Novi Sad, Serbia; tin.lukic@dgt.uns.ac.rs
11 Ruđer Bošković School, Kneza Višeslava 17, 11030 Belgrade, Serbia
* Correspondence: vmc@fb.bg.ac.rs

Abstract

Public health emergency risk assessments commonly summarize likelihood and impact, but categorical risk matrices may not fully represent the population-exposure burden created by multi-hazard portfolios. This nationwide ecological study analyzed municipality-level summaries from 161 Serbian local administrative units assessed with the World Health Organization Strategic Toolkit for Assessing Risks (WHO STAR) in 2024. In addition to the supplied ordinal STAR measures, we derived an analytical probability-impact product (PIP), cumulative hazard-exposure burden (CHEB = hazard count × reported unit-level exposure proportion), exposure-weighted PIP (PIP × exposure), portfolio risk burden (PRB = PIP × CHEB), and a sample-relative 0–100 Integrated Portfolio Disaster Risk Index (IPDRI). Geographic Information Systems (GIS)-based thematic mapping was used to integrate the analytical dataset with local administrative boundaries and to visualize the spatial distribution of the original STAR indicators and derived burden measures. Primary inference combined rank-based methods with Pearson correlations, Welch tests, robust analysis of variance, non-circular sensitivity models, and exploratory cluster analysis. The supplied STAR risk distribution was predominantly moderate (83.2%), with 11.2% low and 5.6% high. Risk was most strongly associated with probability (Spearman's $\varrho = 0.534$, 95% bootstrap CI [0.357, 0.683], $p < 0.001$) and frequency ($\varrho = 0.360$, $p < 0.001$), and differed substantially across 25 districts, $H(24) = 81.95$, $p < 0.001$, $\varepsilon^2 = 0.426$. Applying STAR matrix thresholds to aggregate PIP reproduced the supplied risk

Academic Editor: Raphael Grzebieta

Received: 20 September 2026
Revised: 26 October 2026
Accepted: 30 October 2026
Published: 4 November 2026

Copyright: © 2026 by the authors. Licensee MDPI, Basel, Switzerland. This article is an open access article distributed under the terms and conditions of the Creative Commons Attribution (CC BY) license.

category in 75.8% of units (quadratic weighted $\kappa = 0.484$), indicating only moderate aggregate concordance. IPDRI averaged 43.64 (SD = 21.45) and showed weak, non-significant correspondence with the supplied ordinal STAR risk category (Spearman's $\rho = 0.104$, $p = 0.187$; Kendall's τ-b = 0.084). Its strong Pearson correlation with CHEB ($r = 0.889$, $p < 0.001$) was construction-dependent and did not constitute independent empirical validation of the index. IPDRI differed across macroregions, Welch $F(2, 53.15) = 10.11$, $p < 0.001$, and districts, Welch $F(24, 38.79) = 14.12$, $p < 0.001$. An exploratory three-cluster solution (silhouette = 0.549) identified different local assessment profiles that also differed in the supplied STAR risk category, $F(2, 158) = 12.72$, $p < 0.001$, $\eta^2 = 0.139$. However, these differences represent descriptive within-dataset associations rather than independent external validation. The findings indicate that STAR risk intensity and exposure-weighted portfolio burden capture complementary dimensions of local public health emergency risk and should be interpreted jointly in preparedness planning.

Keywords: public health emergency; WHO STAR; disaster risk assessment; exposure burden; GIS; local government; preparedness; risk typology; Serbia

1. Introduction

Public health emergencies are increasingly understood as manifestations of interacting hazards, exposed populations, pre-existing vulnerability, institutional conditions, and the capacities available to anticipate, absorb, respond to, and recover from disruption. This interpretation is consistent with the broader evolution of disaster-risk science from hazard-centered models toward relational and systems-oriented conceptions of risk, in which adverse outcomes depend on where hazards occur, who and what is exposed, how vulnerability is produced, and which protective capacities are available [1–6]. For public health, the implication is especially important: an identical hazard can generate very different consequences across territories because surveillance, health-service continuity, infrastructure, social protection, risk communication, institutional coordination, and community resources are unevenly distributed.

The all-hazards perspective has therefore become central to preparedness and health security. Public health emergency preparedness is not simply the possession of plans or emergency stockpiles; it is a complex adaptive capability involving governance, leadership, information systems, workforce, partnerships, communication, equity, learning, and the ability to reorganize under stress [7–11]. Health-system resilience similarly requires continuity of essential functions, adaptive reconfiguration, and institutional learning before, during, and after shocks [12–15]. These capacities become particularly consequential when multiple hazards coexist or interact, because preparedness decisions must account not only for the intensity of a single event but also for cumulative exposure, interdependence, and the possibility of cascading consequences.

Contemporary multi-hazard research reinforces this concern. Aggregate, compound, cascading, and systemic risk perspectives show that the total burden of multiple hazards cannot always be inferred from single-hazard assessments considered independently [16–20]. Global disaster-record analyses indicate that multi-hazard events account for a disproportionate share of damages and affected populations, while recent frameworks increasingly emphasize interactions among hazards, infrastructure, governance, and social vulnerability [21–25]. This shift has direct implications for local public health planning, where several moderate hazards may collectively generate substantial operational burden even when no single hazard dominates the risk matrix.

Subnational analysis is consequently indispensable. Local governments and local health systems translate national policy into surveillance, warning, emergency logistics, public communication, service continuity, protection of vulnerable groups, and coordination with civil protection, social services, utilities, civil society, and community organizations. Evidence from different governance settings shows that preparedness and resilience depend strongly on cross-sector collaboration, clarity of mandates, sustained financing, regional coordination, professional networks, and meaningful stakeholder participation [26–32]. Sendai Framework implementation has similarly highlighted persistent difficulties in translating national commitments into locally integrated, data-informed, and accountable disaster-risk governance [33–36].

The World Health Organization (WHO) Strategic Toolkit for Assessing Risks (STAR) operationalizes an all-hazards, whole-of-society approach to strategic public health risk assessment. STAR structures the assessment around hazard identification, probability, impact, vulnerability, coping capacity, data confidence, risk prioritization, and translating findings into preparedness action. Recent applications demonstrate the value of STAR for participatory prioritization and multisector preparedness in different contexts, including Niger State in Nigeria, the WHO Eastern Mediterranean Region, West and Central Africa, and Serbia [37–40]. At the same time, recent evidence also shows that STAR is a strategic assessment tool rather than a statistical forecasting model; its usefulness depends on the quality and timeliness of input data, geographic resolution, expert consensus, and repeated updating [39].

Serbia provides a particularly relevant setting for examining these issues. Previous studies have documented substantial spatial differences in disaster preparedness, resilience, institutional capacity, risk perception, and communication across Serbian municipalities and regions [41–45]. Research following major floods and other hazards has also identified persistent problems related to local preparedness, planning, institutional coordination, public participation, and the uneven translation of policy into practice [46–49]. The national STAR implementation therefore provides an unusual opportunity to examine public-health risk profiles across essentially the full territorial assessment frame rather than a small convenience sample of municipalities.

Research Gap, Methodological Problem, and Study Contribution

Despite rapid growth in indicator-based disaster-risk and resilience assessment, three gaps remain relevant to the present study. First, composite and ordinal indicators can obscure the distinction between risk intensity and cumulative exposure burden. Composite-index research repeatedly shows that different normalization, weighting, aggregation, and spatial-unit decisions can change rankings and policy interpretation [50–54]. Second, formative assessment systems such as STAR contain explicit structural dependencies among variables. In STAR, probability and impact determine the hazard-specific risk category, while impact derives from severity, vulnerability, and coping capacity. Treating these construction components as statistically independent causal predictors of the final score therefore creates part-whole coupling. Third, aggregated municipality-level summaries can create an aggregation-order problem: multiplying an aggregated probability score by an aggregated impact score need not reproduce a risk score first calculated at the hazard level and then aggregated.

The present study addresses these gaps through a nationwide ecological secondary analysis of the Serbian STAR assessments. In addition to the supplied STAR risk category and component scores, the analysis distinguishes probability-impact intensity from exposure-weighted portfolio burden by constructing transparent exploratory measures: the probability-impact product (PIP), cumulative hazard-exposure burden (CHEB), exposure-weighted PIP, portfolio risk burden (PRB), and a sample-relative Integrated

Portfolio Disaster Risk Index (IPDRI). These measures are not proposed as replacements for WHO STAR or as validated expected-loss models. Their purpose is analytical: to test whether a local unit's cumulative portfolio/exposure burden contains information that is not represented by the categorical probability-impact risk matrix.

Consistent with the Sendai Framework's multidimensional understanding of disaster risk, hazard, exposure, vulnerability, and coping capacity should be considered together [23,33,34]. However, this does not imply a universal algebraic formulation requiring capacity to appear as a denominator. The present PRB and IPDRI measures are exploratory portfolio-burden descriptors in which coping capacity is represented indirectly through the supplied STAR impact score rather than independently modeled as a mitigating factor. They should therefore not be interpreted as comprehensive capacity-adjusted measures of disaster risk or community resilience.

To support territorial interpretation of these complementary risk dimensions, the municipality-level analytical data were additionally integrated with administrative spatial units in a GIS environment and visualized through a harmonized set of thematic maps.

Accordingly, the study addresses five questions: (RQ1) What is the national distribution of STAR risk and its component scores across Serbian local administrative units? (RQ2) How are the component scores associated with the ordinal STAR risk level, while recognizing the formative structure of the instrument? (RQ3) How do the supplied STAR indicators and derived burden measures vary across local administrative units and predefined territorial groups, and what geographic distributions are illustrated by thematic mapping? (RQ4) Are the conclusions robust across parametric, robust, ordinal, and nonparametric analyses? (RQ5) Does an exposure-weighted portfolio perspective reveal a complementary dimension of local disaster-related public health burden and empirically distinct local risk profiles?

2. Literature Review and Conceptual Framework

2.1. Disaster Risk as an Interaction of Hazard, Exposure, Vulnerability, and Capacity

Vulnerability scholarship emphasizes that losses arise from the interaction of environmental threats with social, economic, demographic, institutional, and infrastructural conditions [1–3]. In public-health settings, Keim [5] similarly argues that disaster-related health risk requires attention to probability and impact together with the determinants that make populations susceptible or protected. Fine-resolution analyses in Japan, Romania, Italy, Spain, and China demonstrate that exposure and vulnerability vary substantially within countries and that such differences can change the location and magnitude of identified risk [55–59].

Capacity is not simply the conceptual opposite of vulnerability. Empirical and theoretical work has shown that resilience, coping capacity, adaptive capacity, and vulnerability overlap only partially and can produce different territorial rankings [60–62]. A vulnerable community may possess strong social networks or institutional resources, while a less socially vulnerable community may still be poorly prepared for a particular hazard. This distinction is central to public-health emergency management because response depends simultaneously on health-system resources, community networks, information flows, governance, and the ability to mobilize those assets under time pressure [14,63,64].

For this reason, disaster-risk assessment increasingly uses multidimensional frameworks rather than a single hazard score. Marin et al. [6] integrate natural and socioeconomic dimensions; Orencio and Fujii [65] develop a localized resilience index; Mavhura, Manyangadze, and Aryal [66] adapt the Disaster Resilience of Place approach; and Azzimonti, Colleoni, De Amicis, and Frigerio [67] combine hazard, vulnerability, and

resilience for seismic-risk planning. These studies support a conceptual distinction adopted in the present analysis: risk intensity, population exposure, structural susceptibility, and response capacity are related but not interchangeable dimensions and should be interpreted jointly rather than collapsed without qualification.

2.2. From Multi-Hazard Assessment to Compound, Cascading, and Systemic Risk

Multi-hazard assessment encompasses aggregated, compound, cascading, and systemic risks [16–18]. These distinctions matter because aggregate risk rankings can miss interactions, temporal sequences, and feedback mechanisms that alter vulnerability and consequences during a crisis [19,20].

Recent empirical evidence illustrates the magnitude of this problem. Reclassifying historical disasters suggests that multi-hazard events account for a substantial share of disaster losses [21], while analyses of global disaster records found that multi-hazard events were associated with disproportionate shares of total damages, affected populations, and mortality [22]. At the modeling level, dynamic Bayesian networks, event-tree approaches, and multi-hazard asset frameworks increasingly attempt to represent cross-sector dependencies and cascading failures rather than simply summing single-hazard scores [25,68].

This evolution has also shifted the policy debate toward systemic risk governance. Liu and Renn [24] connect systemic-risk and polycrisis scholarship to assessment, governance, and communication; Triyanti et al. [69] show the institutional difficulties of governing cascading risk at the local level; and Tiggeloven et al. [23] identify multiscale coordination, data governance, emerging technologies, and inclusive engagement as priorities for the post-Sendai risk landscape. Adaptive pathway approaches similarly argue that multi-risk management must account for interactions, uncertainty, and changing conditions through time [70].

National-scale applications also demonstrate the practical importance of harmonizing heterogeneous hazard, exposure, and vulnerability information. Delves et al. [71], for example, developed a multi-hazard assessment for Burundi under severe data constraints, emphasizing transparent harmonization and identifying areas where additional data and risk-reduction effort are most needed. Such work supports the present study's emphasis on portfolio burden and data confidence: in a local public-health context, the number of hazards and the share of the population exposed may represent an operational burden not fully captured by the highest or average categorical risk intensity.

Selected applied studies further illustrate how differentiated vulnerability, community preparedness, and recurrent flooding may contribute to uneven local disaster and public-health burdens [72–74]. Canete and Biñas [72] conceptualize differential risk as a function of unequal vulnerability and resilience capacity among elements exposed to the same hazard, while Pradhan, Kumar, and Nayak [73] show how integrated governance, preparedness, and community participation can shift disaster-prone settings from vulnerability toward resilience. Public-health consequences add another layer to this differentiation: Koech [74] links recurrent urban flooding to mortality, displacement, infectious disease, and governance failures, showing how environmental exposure can become a sustained health emergency. Research on technological and industrial hazards further illustrates how natural hazards, industrial vulnerabilities, risk assessment, and emergency planning intersect [75].

2.3. Composite Indicators, Spatial Heterogeneity, and the Problem of Aggregation

Composite indicators are widely used because they translate multiple dimensions into interpretable rankings, maps, and priority classes. However, their apparent simplicity masks important methodological choices. Beccari's [50] review of 106 disaster-risk,

vulnerability, and resilience methodologies found extensive variation in indicator selection, weighting, aggregation, and sensitivity analysis. More recent reviews confirm persistent issues related to context specificity, validation, transferability, and policy use [53,54,76]. Marzi et al. [51] showed that normalization and aggregation affect resilience rankings in Italy; Bucherie et al. [77] found that expert-driven and principal-component approaches can produce different social-vulnerability patterns; and Sibilia et al. [52] demonstrated the value of a multi-level European vulnerability indicator for analyzing change across space and time. These findings caution against interpreting any single composite score as a direct physical quantity.

Spatial resolution further shapes interpretation. Raduszynski and Numada [55] found pronounced submunicipal heterogeneity in Japanese vulnerability and exposure; Chelariu et al. [56] combined geophysical and social vulnerability at the local administrative unit level in Romania; and Galderisi and Limongi [57] emphasized the importance of comprehensive exposure and vulnerability knowledge for risk-informed urban planning. Tascón-González et al. [58] likewise showed how fine-scale vulnerability mapping can support local flood management. GIS thematic maps display geographic differences in hazard, exposure, vulnerability, capacity, and composite indicators. Such spatially explicit approaches are particularly useful when nationally aggregated indicators conceal substantial local heterogeneity [78,79].

These concerns are directly relevant to aggregated STAR data. If probability, impact, and risk are calculated for individual hazards and then separately summarized across the local hazard portfolio, the summary values are not algebraically guaranteed to preserve the original hazard-level scoring relation. The present study therefore treats PIP–STAR disagreement as an aggregation-order diagnostic rather than as proof of error. This approach follows the broader composite-indicator literature in distinguishing a measurement model from the physical or social phenomenon it seeks to represent [50,51,60].

2.4. Public Health Emergency Preparedness, Health-System Resilience, and Strategic Risk Assessment

Public health emergency preparedness has developed from a checklist-oriented concept toward a systems perspective. Nelson, Lurie, Wasserman, and Zakowski [80] emphasized the need for an explicit preparedness construct, while later work conceptualized preparedness as a resilient complex adaptive system of interdependent capacities [7]. Indicator-development research has subsequently operationalized preparedness through measurable capabilities and performance dimensions [81–83].

Health-system resilience scholarship reaches a similar conclusion. Kruk et al. [12] define resilience as preparation, effective response, maintenance of core functions, and reorganization when required. Khatri et al. [8] identify surveillance, integrated services, multisector coordination, digital tools, and resilient system planning as recurring preparedness priorities. In contrast, Gooding et al. [9] show that coordination is enabled by inclusive structures, clear mandates, organizational capacity, and political leadership. Recent assessment instruments further broaden preparedness to include financing, governance, information systems, health-service resources, socioeconomic context, spatial design, and community services [11,84].

Preparedness measurement must also be dynamic. Kandel and Chungong [13] argue for metrics that can change with emerging threats and inform action rather than merely document static capacity. Exercise-based research demonstrates the value of testing communication, information sharing, and organizational roles under simulated pressure [85], while evidence-based preparedness strategies stress emergency procurement,

workforce surge, equity, community partnerships, and the routine use of vulnerability data [15].

WHO STAR fits within this broader risk-based preparedness architecture. It is designed to support systematic hazard prioritization and action planning rather than to produce a purely actuarial prediction. Awoyale et al. [37] showed that a STAR-based multi-hazard assessment can generate actionable state-level preparedness priorities; Elhakim et al. [38] positioned STAR within a wider preparedness ecosystem that includes the International Health Regulations monitoring framework, exercises, emergency operations centers, One Health, and risk communication; and Goode et al. [86] demonstrated the value of structured rapid risk and impact tools for defensible decision-making in environmental emergencies.

Evidence from Serbia and West/Central Africa is especially pertinent. Tomašević et al. [40] described the Serbian local-government STAR process as a capacity-building and harmonization initiative. In contrast, Yota et al. [39] found that STAR's correspondence with observed emergencies varied by hazard and context. Their analysis reinforces a central point for the present study: STAR should be interpreted as a strategic prioritization framework whose performance depends on input data, hazard dynamics, preventive actions, and geographic resolution, not as a fixed statistical forecast. The International Health Regulations address public-health capacities [87]; WHO guidance addresses emergency communication [88]; the WHO Health EDRM Framework integrates health emergency management [89]; and the COVID-19 plan guides pandemic preparedness [90].

The literature also provides directly relevant evidence on the public-health and regional dimensions of risk-informed preparedness. Spatial analysis of notifiable diseases can strengthen the territorial identification of health risk and support geographically differentiated surveillance and intervention [91]. In Southeast Europe, Ivanov [92] identifies coordination gaps, institutional inefficiencies, and resource constraints as ongoing obstacles to implementing disaster risk reduction. International emergency-management research similarly emphasizes the importance of interagency planning, communication, and coordination for effective public preparedness and response [93]. Together, these studies reinforce the rationale for analyzing Serbian STAR results at the subnational level rather than treating national preparedness as spatially uniform.

2.5. Local Governance, Community Resilience, Risk Communication, and Trust

Preparedness is enacted through governance networks rather than by health agencies in isolation. Regionalization can improve resource use, planning, exercises, and professional networks when leadership and trust support it [26]. Conversely, organizational silos between public health, emergency management, local government, and other sectors can weaken preparedness and response [27]. Cross-national governance research similarly identifies collaboration, accountability, multilevel coordination, and locally meaningful participation as recurring determinants of effective disaster-risk governance [29–32].

Sendai implementation research shows that formal policy adoption is insufficient when local capacity, resources, participation, or institutional learning are weak. Mizutori [33] emphasized the importance of disaggregated data, risk-informed investment, and monitoring; Surianto et al. [34] identified persistent gaps in coordination and assessment capacity; Nekoei-Moghadam et al. [35] highlighted the need for context-specific implementation strategies; and Cabral-Ramírez et al. [36] stressed multi-stakeholder co-production. Tiernan et al. [94] similarly observed the growing importance of shared responsibility, public–private partnerships, and adaptive resilience.

At the community level, resilience depends on adaptive capacities, including economic resources, social capital, information and communication, and community

competence [61]. Quantitative operationalization of these capacities has shown that resilience can be assessed with population-level indicators, although contextual interpretation remains essential [62]. Community interventions are more likely to strengthen resilience when they are multi-hazard, participatory, locally grounded, asset-aware, and oriented toward skill development and social connections [63,64,95].

Risk communication is central to this governance architecture. Systematic reviews show that preparedness is enhanced by sustained community engagement, two-way communication, trust, local tailoring, and inclusion rather than by one-way information provision alone [96–98]. Community engagement in early warning remains uneven, particularly across risk knowledge, monitoring, communication, and response capability [99].

Public-health emergency communication research reaches the same conclusion. WHO-informed evidence syntheses identify local stakeholder engagement, interorganizational networks, exercises, and leadership structures as essential for integrating emergency risk communication into preparedness systems [100–102]. COVID-19 further demonstrated how information gaps, infodemics, and insufficient community participation can create additional risk [103,104]. Recent scholarship consequently frames disaster communication as a continuum from dissemination to dialogue and participation [105–107].

Trust links many of these domains. Reviews show that institutional and community trust influence preparedness, warning interpretation, cooperation, and resilience, although effects remain context-dependent [108,109]. This is particularly relevant when risk assessment depends on expert judgment and uneven-quality data: confidence in the evidence base, transparency about uncertainty, and institutional credibility become part of the practical effectiveness of risk governance.

Beyond applied disaster-governance studies, established international theoretical perspectives provide a broader understanding of how social and institutional conditions shape disaster risk. Social-vulnerability scholarship emphasizes that disaster impacts are influenced by socially produced inequalities, access to resources, and underlying development processes [110]. Disaster sociology further demonstrates how organizational decisions, institutional arrangements, and political-economic conditions contribute to the production of risk and resilience [111]. Risk-perception research highlights differences between expert assessments and public judgments of hazards [112], while Cultural Theory of Risk emphasizes the influence of social values and cultural orientations on the selection and prioritization of perceived dangers [113]. Post-normal science advocates broader stakeholder participation when scientific uncertainty is substantial and decision stakes are high [114]. These perspectives provide interpretive foundations for understanding risk governance and communication; they were not directly tested using the present STAR data. Complementary empirical research demonstrates the importance of local governance capacity in fragile settings [115] and the potential divergence between institutional practices and community perspectives on disaster-risk governance [116].

Empirical research on disaster communication complements these theoretical perspectives. Flood early-warning systems can be constrained by institutional, technological, and community-level barriers [117], while school–community collaboration illustrates the importance of locally embedded preparedness relationships [118]. Research on public safety communication highlights the importance of timely and comprehensible warnings [119], and studies of social media and mobile technologies demonstrate their potential contribution to disaster communication and coordination [120]. Emerging technological approaches further emphasize accessibility, risk awareness, and the inclusion of vulnerable populations in disaster preparedness [121].

2.6. Serbia and the Southeast European Evidence Gap

Research in Serbia has documented many of the same structural challenges identified internationally. A national study of local self-government capacity found that effective disaster-risk management required continued development of strategic, operational, financial, partnership, and communication capacity [41]. Household and flood-preparedness research identified low or uneven preparedness and meaningful demographic differences in risk perception and response behavior [46,47]. Policy analysis of the 2014 flood experience highlighted weaknesses in planning, implementation, infrastructure, and risk assessment [48].

More recent Serbian research has moved toward composite resilience and governance analysis. The BRIC–DROP study reported substantial subnational variation and identified risk communication, early warning, evacuation/shelter readiness, and financing as persistent weaknesses [43]. Qualitative research on the evolution of resilience measurement emphasized fragmentation, central dependence, and the limitations of purely indicator-based approaches [44]. The MODERSI framework similarly argues for integrating social identity and community dimensions into resilience assessment [42].

Environmental-risk research in Serbia also shows the importance of trust, transparency, and place-specific governance. Nikolić et al. [45] found that environmental information and institutional transparency were associated with trust and perceived resilience near the Duboko landfill. A wider Southeast European comparison identified limited local capacity, fragmented coordination, and inadequate public awareness as recurring regional challenges despite formal legal and strategic frameworks [49]. These findings make a nationwide local-level public-health risk assessment particularly valuable: it can connect the disaster-resilience literature with the operational risk profiles used for preparedness planning.

The 2024 Serbian STAR implementation provides that opportunity. The national project generated local risk profiles through a standardized participatory methodology across 144 local self-government units and 17 municipalities of the City of Belgrade [40]. The present study extends this operational assessment into a scientific secondary analysis by examining distributional patterns, geographic heterogeneity, scale direction, aggregation effects, and the distinction between probability-impact intensity and cumulative exposure-weighted portfolio burden.

The Serbian and regional literature has also become more explicit about resilience's multidimensionality and measurement limits. International research provides complementary perspectives on the multidimensionality and measurement of community disaster resilience. Cutter et al. [122] developed a place-based conceptual model integrating the social, institutional, economic, and infrastructural conditions shaping community resilience. Subsequent empirical research demonstrated substantial geographic variation in resilience indicators and highlighted the importance of contextual interpretation [123]. Disability-inclusive disaster-risk scholarship further emphasizes accessibility, participation, and institutional support for persons with disabilities [124]. At the critical-infrastructure level, research on interdependent systems demonstrates the importance of accounting for cascading disruptions and infrastructure functionality in risk assessment and preparedness planning [125]. Together, these perspectives support the use of multiple complementary assessment dimensions rather than reliance on a single composite indicator.

3. Methods

3.1. Study Design and Setting

This study used a quantitative, cross-sectional, nationwide ecological design based on secondary analysis of aggregated WHO STAR assessments. The unit of analysis was the local administrative unit. The supplied dataset contained 161 units: 144 local self-government units across Serbia and 17 municipalities of the City of Belgrade. The underlying STAR assessment was implemented from 1 April to 30 September 2024. The official report describes a participatory, evidence-informed assessment process involving public health institutes, local governments, health services, emergency-management structures, and other relevant actors [40]. Importantly, the 161 administrative units were not necessarily equivalent in territorial size, population, administrative responsibilities, institutional organization, or hazard-identification opportunities. In particular, the 17 municipalities within the City of Belgrade differ administratively from the 144 other local self-government units included in the dataset. These differences may influence the number of identified hazards, reported population exposure, and the resulting aggregated assessment scores. Accordingly, the local administrative unit was treated as the observational unit available in the source dataset rather than as a spatially standardized or functionally equivalent unit. All geographic and administrative-group comparisons were therefore interpreted descriptively, recognizing that differences in administrative scale and institutional context could contribute to observed variation.

3.2. STAR Measures and Coding

The analysis used nine municipality-level variables: number of identified hazards, exposure, frequency, probability, impact, coping-capacity score, vulnerability, data-confidence level, and overall risk level. Exposure was represented by the reported unit-level exposure proportion (e_i), expressed on a 0–1 scale. The available dataset does not establish whether this measure represents an average across hazards or the proportion of unique residents exposed. Frequency, probability, impact, coping capacity, vulnerability, confidence, and risk were ordinal STAR-derived scores. In the official STAR capacity coding, 1 indicates very high coping capacity and 5 very low coping capacity; thus, higher numeric capacity scores represent weaker capacity. In the supplied data, the observed capacity range was 2–4. Vulnerability ranged from 2 to 3, confidence from 2 to 3, impact from 2 to 3, and risk from 2 to 4.

STAR impact is a derived score based on severity, vulnerability, and coping capacity, while the hazard-specific risk level is generated through a 5 × 5 risk matrix based on probability × impact. The supplied research spreadsheet contained one aggregate score per local administrative unit. Municipality-level STAR profiles were operationalized using the component scores and overall risk categories available for each local assessment. These measures were analyzed as the primary indicators of the local risk profile, while additional composite indices developed in this study were calculated as exploratory analytical extensions using partly overlapping components of the same assessment dataset. The derived measures were therefore interpreted as analytical extensions of the STAR framework rather than as direct reproductions of the original risk-classification procedure.

3.3. Data Quality Control

The spreadsheet was checked programmatically before analysis. All 161 local administrative units were unique, and no duplicate district-unit combinations were found. One exposure entry for Golubac was stored as the text string “23.80%”; it was normalized to the numeric proportion 0.238. After this correction, all nine analytic variables had N =

161. Four columns intended to represent managerial, health-sector, non-health-sector, and community subcapacities contained only zeros and therefore had no variance; they were excluded from inferential analysis. These zero-only entries were treated as non-informative fields rather than evidence that the corresponding capacities were absent or identical across administrative units. The available source documentation did not establish whether the zeros represented assessed values, unrecorded information, or data omitted during export. The complete analysis-ready municipality-level dataset, including the original STAR indicators, derived portfolio-burden measures, risk classifications, and exploratory cluster assignments for all 161 local administrative units, is provided in Supplementary Tables S5 and S6.

3.4. Statistical Analysis

The primary analysis respected the ordinal nature and restricted range of the STAR scores. We reported frequencies and percentages for categorical/ordinal variables; we retained means and standard deviations as descriptive summaries to facilitate comparison, but used medians and interquartile ranges for ordinal interpretation. Spearman rank correlations were calculated between risk and the other variables, with 3000 nonparametric bootstrap resamples for 95% confidence intervals. Kendall's tau-b was calculated as a sensitivity measure for tied ordinal data. Holm adjustment was applied across the complete set of pairwise correlations. Spearman's rank correlation coefficient (ϱ) was designated as the primary measure of association whenever at least one variable was an ordinal STAR assessment score. Kendall's tau-b (τ-b) was used as a supplementary sensitivity measure to account explicitly for tied observations resulting from the restricted ordinal scales. Pearson's product–moment correlation coefficient (r) was reserved for supplementary analyses involving sufficiently continuous variables, including appropriate comparisons among derived portfolio-burden measures. Correlations involving mathematically related indicators were interpreted cautiously because shared components could induce associations independently of substantive empirical relationships.

Regional heterogeneity was assessed across 25 districts/territorial groups using Kruskal–Wallis tests for each analytic variable. Epsilon-squared (ε^2) quantified effect size, and Holm correction was applied across the nine omnibus regional tests. Where the omnibus test for risk was significant, Dunn pairwise comparisons with Holm correction were used. The association between district and the three observed risk categories (low, moderate, high) was also examined with a Pearson chi-square statistic; because 65 expected cells were below 5, statistical significance was evaluated with 5000 label permutations, and a bias-corrected Cramér's V quantified association strength.

Ordinary least-squares (OLS) regression was retained exclusively as a secondary sensitivity and descriptive decomposition analysis rather than a primary inferential approach. The dependent variable was the supplied ordinal STAR risk category, treated numerically for the purposes of this sensitivity analysis. This specification assumes approximately equal distances between adjacent risk categories, an assumption that cannot be established for the STAR ordinal scale. Furthermore, several predictors are mathematically or conceptually embedded in the STAR risk construction, introducing formative dependence between predictors and the outcome. Hierarchical OLS models were estimated using heteroskedasticity-consistent HC3 standard errors, and model diagnostics included variance-inflation factors, Breusch–Pagan and White tests, residual-normality assessments, Ramsey RESET, leverage, and Cook's distance.

Although HC3 standard errors address heteroskedasticity-related inference, they do not resolve ordinal measurement limitations, formative dependence, or potential model misspecification. Consequently, the OLS results were interpreted as supplementary

sensitivity findings rather than causal effects, independent risk determinants, or external validation of the STAR assessment framework. First, the hierarchical ordinary least-squares models were re-estimated after correcting the exposure value and using heteroskedasticity-consistent HC3 standard errors. Variance-inflation factors, Breusch–Pagan and White tests, residual normality diagnostics, Ramsey RESET, leverage, and Cook's distance were examined. Second, cumulative-logit ordinal models were estimated using standardized predictors.

These models were retained to assess robustness of the original analytical strategy, but coefficient interpretation explicitly recognizes STAR's formative construction. Complementary sensitivity models and derived portfolio-burden analyses are described separately below. The cumulative-logit models were interpreted as sensitivity analyses under the proportional-odds assumption. Particular caution was applied because the highest observed STAR risk category contained only nine administrative units and several predictors were formative components of the risk-classification framework. The resulting odds ratios were therefore interpreted as conditional associations with the supplied ordinal assessment categories rather than changes in the probability of actual emergency occurrence.

3.5. Derived Burden Variables and Complementary Analyses

Two additional models were specified to avoid direct part-whole coupling. First, the analytical PIP score was regressed on CHEB, data confidence, and macroregion indicators using HC3 robust standard errors; probability, impact, vulnerability, and coping capacity were deliberately excluded as predictors. Second, an exploratory cumulative-logit model estimated the association of the supplied STAR risk category with CHEB, data confidence, and macroregion. Separately, we calculated two additional descriptive composites: structural susceptibility, defined as the mean of vulnerability and the inverse-coded coping-capacity score, and hazard dynamics, defined as the mean of frequency and probability.

For complementary portfolio-burden analysis, we calculated five transparent derived variables. For each local administrative unit i, PIP_i was calculated as the product of the supplied unit-level probability score (P_i) and impact score (I_i). Because the supplied municipality-level STAR risk category was not always reproduced by thresholding this unit-level cross-product, we treated PIP as an analytical consistency score rather than the official risk measure. CHEB was calculated as $CHEB_i = H_i \times e_i$, where H_i denotes the number of identified hazards and e_i the reported unit-level exposure proportion. CHEB is a dimensionless descriptor of nominal cumulative hazard exposure, not a percentage or count of uniquely exposed residents. Because the same individuals may be exposed to multiple hazards, CHEB values exceeding 1 do not imply that more than 100% of distinct residents are exposed. The available summaries do not permit identification or correction of overlapping exposed populations. Exposure-weighted PIP was PIP × exposure. PRB was defined as PIP × CHEB, thereby combining the supplied unit-level probability–impact cross-product with hazard count and the reported unit-level exposure proportion. Coping capacity was not introduced as a separate mitigating divisor because the supplied STAR impact score already incorporates a coping-capacity component, and the capacity indicator is an inversely coded ordinal score (1 = very high capacity; 5 = very low capacity). Dividing PRB by the original capacity score would incorrectly reduce the calculated burden as coping capacity deteriorates, whereas using a recoded denominator would require unsupported ratio-scale assumptions and could duplicate the capacity contribution already represented in STAR impact. Accordingly, PRB and its normalized derivative, IPDRI, were treated as exploratory portfolio-burden descriptors rather than comprehensive capacity-adjusted risk measures. PRB was transformed into the

exploratory Integrated Portfolio Disaster Risk Index (IPDRI) using min–max normalization across the 161 administrative units (IPDRI = 100 × [PRB − minimum PRB]/[maximum PRB − minimum PRB]). Accordingly, IPDRI represents a sample-relative measure of constructed portfolio burden under the specified analytical framework rather than a general or externally calibrated risk index. Values of 0 and 100 correspond exclusively to the lowest and highest observed PRB values within the analyzed sample and do not indicate the absence of risk or the maximum possible level of disaster risk. The resulting scores and administrative-unit rankings are conditional on the dataset, indicator construction, and normalization procedure and should not be interpreted as absolute risk estimates, expected losses, or official WHO STAR classifications. We summarized structural susceptibility as the mean of vulnerability and the official inverse-coded coping-capacity score, and hazard dynamics as the mean of frequency and probability.

An important methodological distinction was made between mathematical relationships among constructed indicators, descriptive empirical associations, and independent external validation. PIP was calculated from the supplied probability and impact scores, CHEB from hazard count and the reported exposure proportion, and PRB as the product of PIP and CHEB. IPDRI was subsequently obtained through a sample-relative linear rescaling of PRB. Consequently, associations among these indicators are partly determined by their shared mathematical components. In particular, IPDRI and PRB are mathematically equivalent up to linear transformation, whereas associations between IPDRI and CHEB are partly induced by the inclusion of CHEB in the PRB formula. Such associations describe the internal structure of the constructed measures and do not constitute independent empirical validation. External validation would require independently observed outcomes, such as emergency activations, morbidity, mortality, economic losses, or health-service disruptions, which were not available in the present dataset. Index-construction sensitivity was assessed by comparing baseline PRB rankings with five alternatives: exposure-weighted PIP without hazard count, three additive combinations of separately min–max normalized PIP and CHEB (50:50, 25:75, and 75:25), and CHEB alone. Spearman rank correlations and top-20 overlap were calculated using the rounded supplementary-table values.

Associations involving ordinal STAR indicators were primarily examined using Spearman's rank correlation coefficient (ϱ), with Kendall's tau-b (τ-b) serving as a sensitivity check for tied observations. Pearson's correlation coefficient (r) was retained as a supplementary measure for associations between sufficiently continuous derived variables, with Fisher's z-transformation used to construct 95% confidence intervals for Pearson correlations. Holm adjustments were applied within explicitly defined families of correlation tests. Because several derived indicators shared mathematical components, their correlations were interpreted descriptively rather than as independent validation evidence. Pre-specified two-group comparisons used Welch independent-samples t tests, Hedges' g, and Mann–Whitney U sensitivity tests for: data confidence score 3 versus 2, Belgrade versus all other units, and Vojvodina versus Central Serbia. We examined macroregional and district differences with classical and Welch ANOVA where estimable, supplemented by Kruskal–Wallis tests and nonparametric effect sizes. Pairwise district contrasts used Welch tests with Holm correction. We quantified agreement between the PIP-based risk-matrix category and the supplied STAR risk category using exact agreement and linearly/quadratically weighted Cohen's κ. Finally, K-means clustering was conducted as an explicitly exploratory procedure to identify descriptive local assessment profiles rather than validated risk classifications. Four variables were standardized before clustering: frequency, CHEB, vulnerability, and coping-capacity score (where higher scores indicate poorer capacity). Candidate solutions with $k = 2–6$ were examined, with the silhouette coefficient used as the primary criterion for selecting

the number of clusters. To assess internal reproducibility and sensitivity to clustering methodology, additional analyses were conducted using the rounded municipality-level values reported in Supplementary Tables S5 and S6. The reference K-means solution was estimated using 50 initializations and a fixed random seed (20261021). Its partition was compared with the reported cluster membership using the adjusted Rand index (ARI), which is invariant to cluster-label permutations. A three-cluster hierarchical solution using Ward's linkage was also estimated from the same standardized variables and compared with the K-means partition. These procedures assessed internal consistency and algorithmic sensitivity rather than external validity or the existence of natural risk groups.

Although the supplied STAR risk category was not directly included among the K-means clustering variables, it was not treated as an independent external validation criterion. The clustering inputs included frequency, CHEB, vulnerability, and coping-capacity scores, several of which share direct or indirect construction pathways with the supplied STAR risk category. Specifically, frequency contributes to probability assessment, vulnerability and coping capacity contribute to impact, and probability and impact determine the hazard-specific STAR risk classification. Consequently, comparisons between cluster membership and the supplied STAR risk category were interpreted exclusively as descriptive within-dataset profile comparisons. Associations with PIP and IPDRI were subject to similar limitations arising from shared mathematical components. No independent external validation was performed.

Cluster stability was evaluated using two complementary procedures to distinguish sensitivity to algorithm initialization from sensitivity to changes in the analyzed observations. First, a reference K-means solution with three clusters was estimated using z-standardized frequency, CHEB, vulnerability, and coping-capacity scores, with 50 random initializations and a fixed random seed (20261021). The analysis was then repeated 100 times using different random seeds, with 50 initializations per fit. Agreement with the reference partition was evaluated using the adjusted Rand index (ARI). Second, observation-level stability was examined through 500 random subsamples comprising 80% of the administrative units (n = 129), drawn without replacement within each iteration. Standardization was recalculated separately for each subsample, and K-means clustering was repeated with 20 initializations. ARI values were calculated by comparing each subsample partition with the reference cluster labels for the same administrative units. Stability was summarized using the median ARI and empirical 2.5th–97.5th percentiles. These percentiles describe the observed distribution of resampling results rather than a confidence interval for population-level cluster validity. All additional stability analyses used the rounded values reported in Supplementary Tables S5 and S6.

3.6. GIS-Based Spatial Data Integration and Thematic Mapping

GIS methods were applied to integrate the municipality-level analytical dataset with the corresponding administrative spatial units and to support the spatial interpretation of the WHO STAR indicators and the derived risk-burden measures. We performed spatial processing and thematic mapping in QGIS version 3.44 using an administrative boundary dataset. All spatial layers were processed in a common coordinate reference system (EPSG:8682).

The analytical database was linked to the administrative boundary layer using consistent local administrative unit identifiers. Before the spatial join, attribute and spatial records were harmonized for administrative-unit names, territorial correspondence, diacritical characters, and dataset structure. Record matching was subsequently verified to ensure one-to-one correspondence between the analytical observations and the mapped local administrative units. For administrative units without analytical observations, we

retained them as spatial context and explicitly represented them as "No data"; we did not spatially interpolate or estimate missing analytical values.

We prepared thematic maps for the supplied WHO STAR risk level and its selected components, as well as for the derived exposure-weighted and portfolio-burden measures. Categorical and ordinal indicators were mapped according to their observed score categories, whereas continuous and count-based variables were represented using graduated classes selected according to their empirical distributions; the exact class boundaries are reported in the corresponding map legends. We applied a harmonized cartographic framework across the map series for administrative boundaries, symbology, labels, spatial extent, and missing-data representation. Because the 17 City of Belgrade municipalities are densely packed, an enlarged inset was included to preserve the visibility of individual administrative units and their numerical labels.

The GIS component was used exclusively for descriptive geographic visualization rather than inferential spatial analysis. The thematic maps illustrated the geographic distribution and variation in the supplied STAR indicators and derived portfolio-burden measures across the 161 local administrative units. They were not intended to identify statistically significant spatial clusters, hotspots, or spatial autocorrelation. No global Moran's I, local indicators of spatial association (LISA), or spatial scan statistics were calculated. Furthermore, the Kruskal–Wallis and Welch tests used elsewhere in the study assessed differences between predefined administrative groups rather than spatial dependence. Similarly, K-means clustering classified administrative units according to similarities in their assessment attributes and did not constitute geographic clustering. Accordingly, all mapped patterns were interpreted descriptively, without inferring statistically significant spatial dependence.

3.7. Visual Overview of the Research Workflow

This subsection visually summarizes how the study was operationalized, from the initial source materials to the final analytic outputs. The figures are not decorative additions; they clarify the logic of the research design, the relationship between the official WHO STAR framework and the derived variables, and the sequence of statistical procedures.

To improve methodological transparency, we added three visual workflow figures. Figure 1 summarizes the overall research process, Figure 2 explains the analytical structure of the official and derived measures, and Figure 3 presents the sequence of statistical procedures used to obtain the final findings.

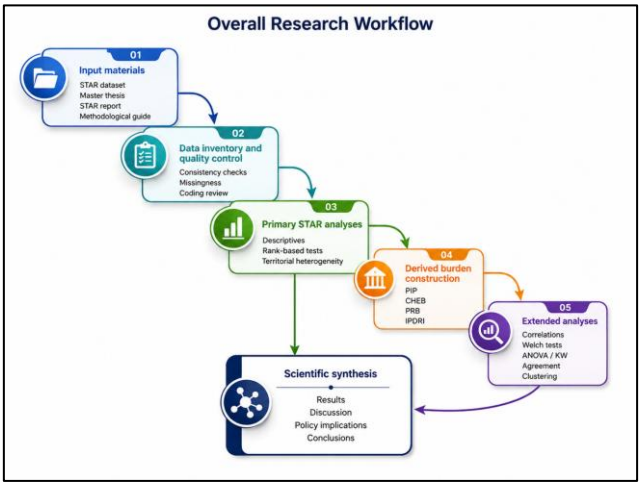


Figure 1. Overall research workflow, from source materials and data quality control to primary STAR analyses, derived-variable construction, extended analyses, and scientific synthesis.

Figure 2 clarifies the study's analytical logic. The official STAR stream is organized around hazard occurrence, frequency, probability, severity, vulnerability, coping capacity, impact, and the resulting risk intensity. In parallel, the present study constructed complementary portfolio-burden measures—PIP, CHEB, PRB, and IPDRI—to distinguish probability–impact intensity from broader exposure-weighted burden.

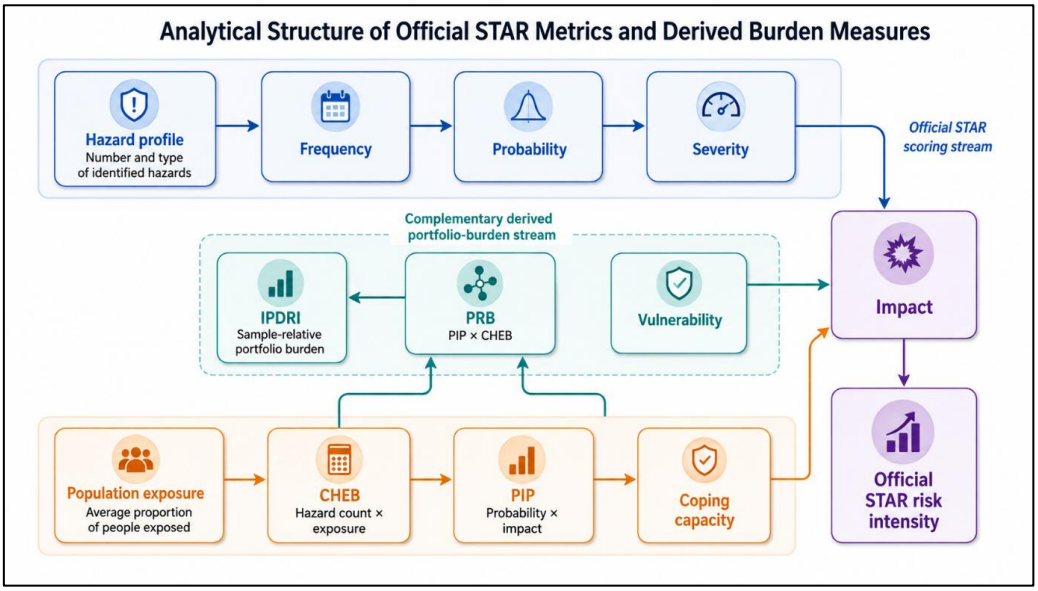


Figure 2. Analytical structure of the official STAR metrics and the complementary derived burden measures used in the study.

Figure 3 synthesizes the statistical workflow. The analysis began with dataset preparation and descriptive profiling, continued with rank-based and territorial comparisons of the official STAR variables, and then moved to constructing and testing derived portfolio-burden measures. The final stage integrated the outputs into tables, figures, and manuscript interpretation.

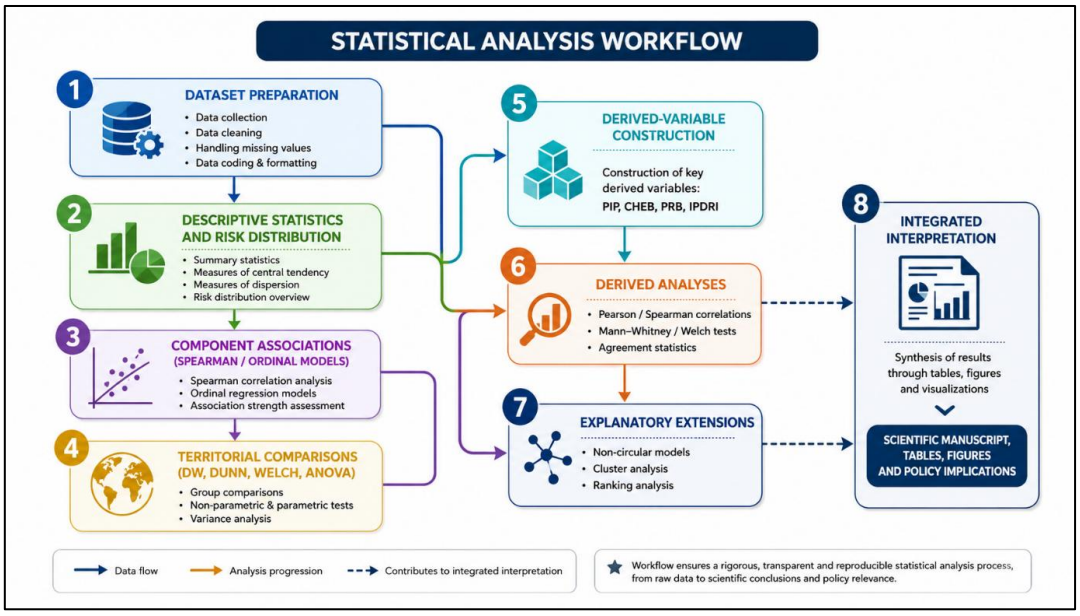


Figure 3. Statistical analysis workflow showing the sequence of descriptive, inferential, derived-variable, and exploratory procedures used in the study.

3.8. Literature Evidence Synthesis

To strengthen the theoretical framing and interpretation of the empirical results, the team conducted a targeted narrative evidence synthesis on 1 September 2026. Searches covered multi-hazard and systemic risk, public-health emergency preparedness, health-system resilience, composite vulnerability/resilience indices, local disaster governance, risk communication, community engagement, and Serbian disaster-risk research. This literature component is a focused narrative synthesis rather than a PRISMA systematic review and is not presented as an exhaustive estimate of the global evidence base.

4. Results

The results are presented in three analytical stages: primary assessment analyses, complementary and sensitivity analyses, and final exploratory clustering.

4.1. Data Characteristics and National Risk Distribution

Municipality-level values for all 161 local administrative units are reported in Supplementary Table S5. The complete supplementary statistical results are presented in Supplementary Tables S1–S6,, while additional GIS-based thematic maps are provided in Supplementary Figures S1–S10. The mean number of identified hazards was 11.04 (SD = 1.67; median = 10; range = 8–18). Mean exposure was 25.6% (SD = 10.3%; median = 26.4%; range = 1.9–48.5%). Most ordinal component scores were concentrated around level 3, indicating substantial range restriction: frequency M = 3.04, probability M = 3.01, impact M = 2.72, coping-capacity score M = 2.95, vulnerability M = 2.91, and data confidence M = 2.19. Table 1 summarizes descriptive statistics for all nine analytic variables. The municipality-level spatial distribution of the identified hazard count is provided in Supplementary Figure S1.

The overall risk distribution was strongly concentrated at the moderate level. Of the 161 units, 134 (83.2%) had risk level 3, 18 (11.2%) had risk level 2, and 9 (5.6%) had risk level 4. No units in the analytic spreadsheet were assigned levels 1 or 5.

Table 1. Descriptive characteristics of the municipality-level STAR dataset.

Variable	Mean	SD	Median	IQR	Range
Hazard count	11.04	1.67	10	10–12	8–18
Exposure proportion	0.256	0.103	0.264	0.182–0.318	0.019–0.485
Frequency score	3.04	0.52	3	3–3	2–4
Probability score	3.01	0.40	3	3–3	2–4
Impact score	2.72	0.45	3	2–3	2–3
Coping-capacity score	2.95	0.29	3	3–3	2–4
Vulnerability score	2.91	0.28	3	3–3	2–3
Data-confidence score	2.19	0.40	2	2–2	2–3
Risk level	2.94	0.41	3	3–3	2–4

Note. N = 161 for all variables after normalization of the Golubac exposure entry. Higher coping-capacity scores indicate poorer coping capacity under official STAR coding. Vulnerability and impact scores were restricted to observed values of 2 and 3, while several other ordinal scores were concentrated around level 3. This restricted variation limits score discrimination and produces tied observations in subsequent analyses.

The thematic maps provide a descriptive representation of the geographic distribution of STAR indicators across the analyzed administrative units, complementing the national descriptive statistics without implying statistically significant spatial clustering or autocorrelation. The moderate WHO STAR risk category is geographically

widespread, whereas low- and high-risk classifications occur in a more limited number of local administrative units (Figure 4A). Probability scores similarly show a predominance of the intermediate category, with higher and lower values occurring more selectively across the country (Figure 4B). In contrast, population exposure shows substantially greater local spatial variability, indicating that administrative units with similar risk or probability scores may differ markedly in the proportion of the population exposed (Figure 4C).

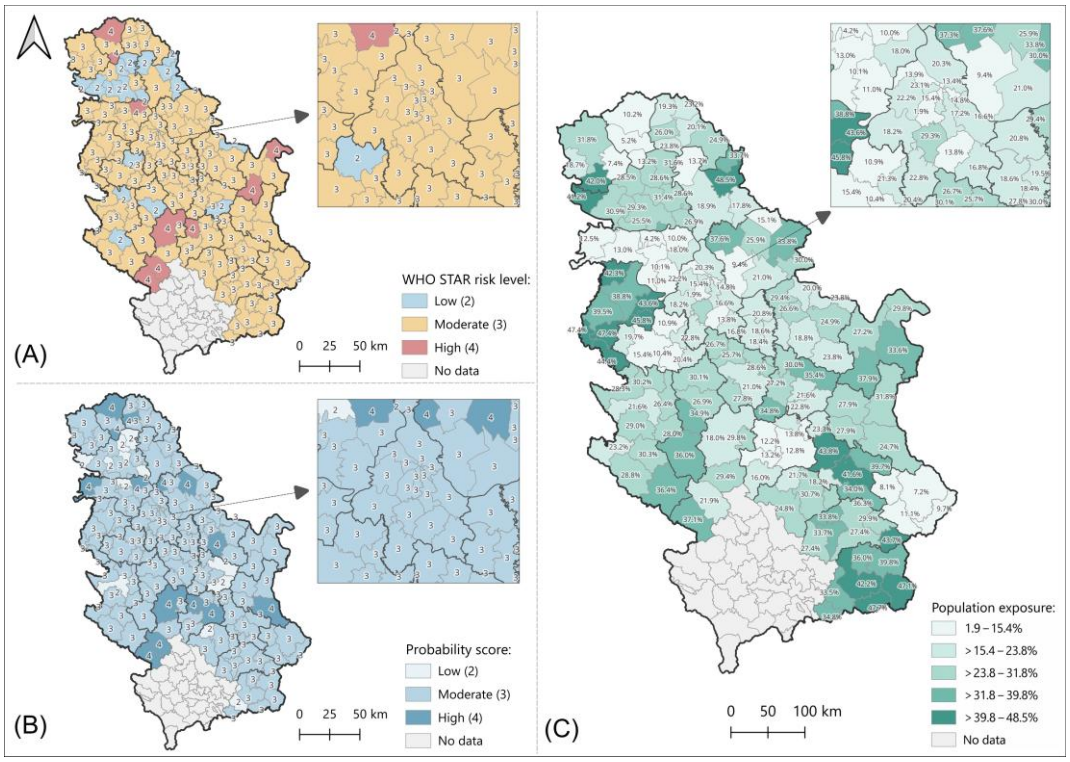


Figure 4. Spatial distribution of selected WHO STAR public health risk characteristics across Serbian local administrative units: (**A**) supplied WHO STAR risk level; (**B**) probability score; and (**C**) population exposure. The inset enlarges the City of Belgrade to preserve the visibility of its 17 city municipalities. Areas outside the analytical dataset are shown as No data. The maps are descriptive and do not imply statistically significant spatial clustering or autocorrelation.

4.2. Associations Between Star Components and Risk Level

Rank-based analysis showed the strongest positive association between risk level and probability ($\varrho = 0.534$, 95% bootstrap CI [0.357, 0.683], $p < 0.001$), followed by frequency ($\varrho = 0.360$, 95% CI [0.221, 0.499], $p < 0.001$). Vulnerability was also positively associated with risk, $\varrho = 0.287$, 95% CI [0.090, 0.478], $p < 0.001$, as was impact, $\varrho = 0.258$, 95% CI [0.093, 0.409], $p = 0.001$. The numeric coping-capacity score had a positive association with risk, $\varrho = 0.240$, $p = 0.002$; because higher STAR capacity scores indicate poorer coping capacity, the substantive direction is consistent with weaker capacity accompanying higher risk. After Holm adjustment across all pairwise correlations, risk remained significantly associated with probability, frequency, vulnerability, and impact, whereas the capacity association did not. The municipality-level spatial distributions of frequency, impact, coping-capacity, and vulnerability scores are shown in Supplementary Figures S2–S5, respectively.

Exposure showed a small negative association with risk that did not reach conventional significance ($\varrho = -0.139$, $p = 0.079$). Hazard count ($\varrho = 0.049$, $p = 0.538$) and data confidence ($\varrho = -0.046$, $p = 0.561$) were not associated with risk. Kendall tau-b results

were directionally consistent with the Spearman analysis. Table 2 presents full rank-based association estimates.

As a complementary risk-category profile analysis, Kruskal–Wallis tests across low, moderate, and high risk categories showed differences in frequency, probability, impact, vulnerability, and coping-capacity score after Holm adjustment (adjusted p-values ≤ 0.039). In contrast, hazard count, exposure, and data confidence did not differ significantly (adjusted p-values ≥ 0.610). The largest category-separation effect was observed for probability ($\varepsilon^2 = 0.307$), followed by frequency ($\varepsilon^2 = 0.128$) and vulnerability ($\varepsilon^2 = 0.087$). Because probability and impact are embedded in STAR risk construction, and vulnerability and coping capacity contribute to impact, these contrasts are descriptive profile checks rather than independent explanatory tests; we report full results in the supplementary statistical workbook.

Table 2. Rank-based associations with the ordinal risk level.

Variable	Spearman ϱ	95% Bootstrap CI	p	Holm-Adjusted p	Kendall τb
Probability	0.534	[0.357, 0.683]	<0.001	<0.001	0.523
Frequency	0.360	[0.221, 0.499]	<0.001	<0.001	0.346
Vulnerability	0.287	[0.090, 0.478]	<0.001	0.007	0.282
Impact	0.258	[0.093, 0.409]	0.001	0.029	0.253
Coping-capacity score	0.240	[0.051, 0.423]	0.002	0.061	0.235
Exposure	−0.139	[−0.283, 0.020]	0.079	1.000	−0.112
Hazard count	0.049	[−0.100, 0.191]	0.538	1.000	0.043
Data confidence	−0.046	[−0.177, 0.074]	0.561	1.000	−0.045

Note. Bootstrap confidence intervals used 3000 resamples. Holm adjustment shown here derives from all pairwise correlations among the nine analytic variables—higher coping-capacity score = poorer capacity.

4.3. Regional Heterogeneity

All nine analytic variables differed significantly across the 25 districts/territorial groups after Holm correction. The largest regional effects were observed for data confidence, $H(24) = 118.47$, $p < 0.001$, $\varepsilon^2 = 0.695$; exposure, $H(24) = 109.97$, $p < 0.001$, $\varepsilon^2 = 0.632$; hazard count, $H(24) = 103.30$, $p < 0.001$, $\varepsilon^2 = 0.583$; vulnerability, $H(24) = 94.29$, $p < 0.001$, $\varepsilon^2 = 0.517$; and frequency, $H(24) = 93.57$, $p < 0.001$, $\varepsilon^2 = 0.512$. Risk level itself showed a large regional effect, $H(24) = 81.95$, $p < 0.001$, $\varepsilon^2 = 0.426$. The corresponding district-level heterogeneity statistics are summarized in Table 3. The municipality-level maps in Supplementary Figures S1–S5 provide spatial context for these statistically identified territorial differences.

The district-by-risk contingency table produced $\chi^2(48) = 150.20$. Because most expected counts were sparse, we did not rely on the asymptotic chi-square p-value; the 5000-permutation Monte Carlo test remained significant ($p < 0.001$), and the bias-corrected Cramér's V was 0.566, indicating substantial differences in the distribution of STAR risk categories among predefined administrative districts, without establishing spatial autocorrelation or statistically significant geographic clustering. Mean risk was highest in North Bačka (M = 3.67; n = 3), Raška (M = 3.60; n = 5), and Bor (M = 3.50; n = 4), while Central Banat (M = 2.20; n = 5) and South Bačka (M = 2.33; n = 12) had the lowest means. Figure 5 shows the district-level composition of low, moderate, and high STAR risk categories, ordered by mean risk level. Interpret these descriptive district rankings cautiously because several districts contained few units.

Table 3. Regional heterogeneity across STAR variables.

Variable	Kruskal–Wallis H	*p*	Holm-Adjusted *p*	ε^2
Data confidence	118.47	<0.001	<0.001	0.695
Exposure	109.97	<0.001	<0.001	0.632
Hazard count	103.30	<0.001	<0.001	0.583
Vulnerability	94.29	<0.001	<0.001	0.517
Frequency	93.57	<0.001	<0.001	0.512
Coping-capacity score	86.64	<0.001	<0.001	0.461
Risk level	81.95	<0.001	<0.001	0.426
Impact	61.88	<0.001	<0.001	0.279
Probability	56.19	<0.001	<0.001	0.237

Note. df = 24 for all tests. Epsilon-squared is reported as the nonparametric effect-size estimate—higher coping-capacity score = poorer capacity.

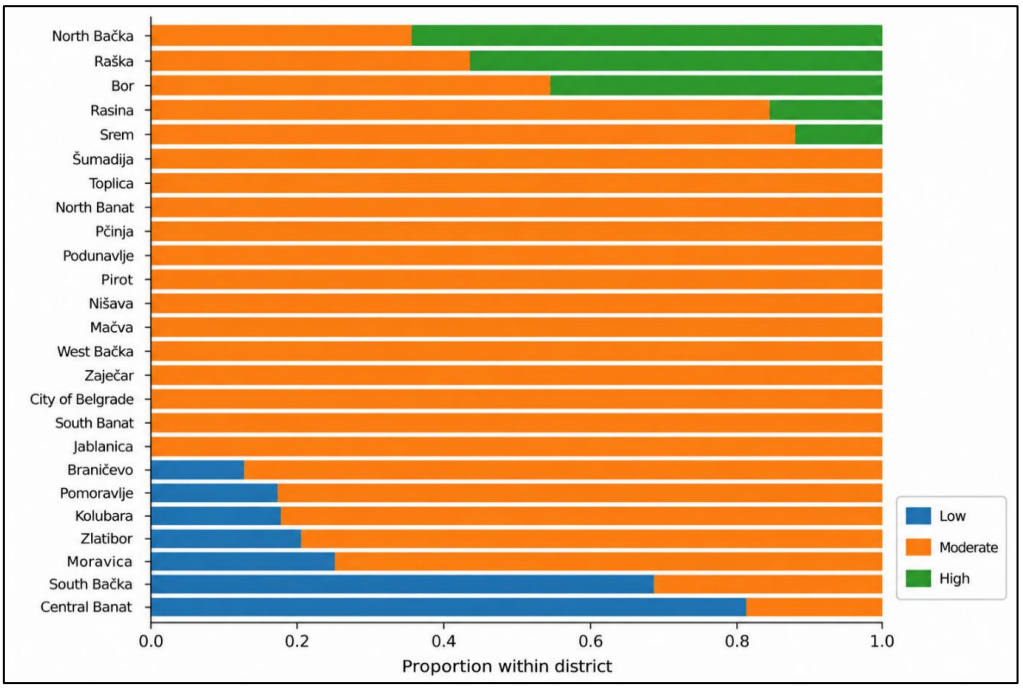


Figure 5. District-level composition of low, moderate, and high aggregated public health risk categories, ordered by mean risk level.

4.4. Pairwise Regional Contrasts for Risk

Dunn–Holm post hoc tests identified 12 statistically significant district pairs for risk. South Bačka had lower risk ranks than Belgrade, Rasina, Raška, Srem, North Bačka, and Bor. Central Banat had lower risk ranks than Rasina, Raška, Srem, North Bačka, and Bor. The strongest contrast was between South Bačka and Raška (Holm-adjusted $p < 0.001$). Table 4 reports the 12 statistically significant Dunn–Holm district contrasts. Full post hoc results for all regional component comparisons are provided in the supplementary statistical workbook.

Table 4. Significant Dunn–Holm pairwise comparisons for risk level.

District 1	District 2	z	Holm *p*
City of Belgrade	South Bačka	4.44	0.003
City of Belgrade	Central Banat	3.95	0.023
South Bačka	Rasina	−4.13	0.010
South Bačka	Raška	−5.80	<0.001

South Bačka	Srem	−4.23	0.007
South Bačka	North Bačka	−5.03	<0.001
South Bačka	Bor	−4.94	<0.001
Rasina	Central Banat	3.97	0.021
Raška	Central Banat	5.41	<0.001
Srem	Central Banat	4.01	0.018
North Bačka	Central Banat	4.90	<0.001
Bor	Central Banat	4.75	<0.001

Note. Two-sided Dunn tests with Holm correction across all 300 district pairs for risk.

4.5. Model-Based Sensitivity Analyses

The following model-based analyses were retained exclusively as supplementary sensitivity analyses to assess the consistency of the primary findings under alternative statistical specifications. Given the ordinal nature of the supplied STAR risk category, primary interpretation was based on descriptive statistics, rank-based associations, and appropriate nonparametric comparisons. The hierarchical OLS models were treated as descriptive decomposition analyses because their numerical specification assumes approximately equal distances between ordinal risk categories, while several predictors are embedded in the STAR risk construction. Consequently, the regression coefficients and model fit were not interpreted as evidence of independent causal determinants, predictive validity, or external validation of the STAR framework.

The full M3 model explained 48.2% of the variance in the numeric risk score (R^2 = 0.482, adjusted R^2 = 0.455). With HC3 standard errors, probability (B = 0.483, β = 0.479, p < 0.001), frequency (B = 0.137, β = 0.176, p = 0.007), vulnerability (B = 0.347, β = 0.241, p = 0.018), and impact (B = 0.171, β = 0.189, p = 0.016) were positively associated with risk. Exposure was negatively associated with risk (B = −0.500, β = −0.126, p = 0.018). The coping-capacity score, hazard count, and data confidence were not independently significant. Full M3 coefficient estimates based on HC3 robust standard errors are reported in Table 5. Adding exposure and capacity to M1 increased R^2 by 0.020 (nested p = 0.061), and adding hazard count and confidence to M2 increased R^2 by 0.015 (nested p = 0.109).

The full-model VIFs ranged from 1.13 to 1.31, indicating no material multicollinearity. Breusch–Pagan and White tests did not indicate heteroskedasticity, but residual normality was rejected (Shapiro–Wilk W = 0.939, p < 0.001; Jarque–Bera p < 0.001). Twenty observations exceeded the conventional Cook's distance threshold of 4/N, reinforcing the decision to treat OLS as a sensitivity analysis. A Brown–Forsythe regional comparison remained significant, p < 0.001. The standardized cumulative-logit sensitivity model indicated a positive association between the probability score and the supplied STAR risk category (OR = 5.038, 95% CI [2.809, 9.036], p < 0.001). Under the proportional-odds specification, this estimate represented the fitted cumulative odds of belonging to a higher STAR risk category for each one-standard-deviation increase in the probability score, conditional on the other model predictors. Importantly, this result did not imply a fivefold increase in the probability of an actual emergency or disaster event. Only nine administrative units (5.6%) belonged to the highest observed risk category (level 4), limiting the information available for estimating upper-category contrasts and warranting caution regarding model sensitivity and generalizability. Furthermore, probability is a formative component of the STAR risk-classification framework, meaning that the estimated association partly reflects the instrument's construction. Therefore, the magnitude of the odds ratio was not interpreted as an independent causal or predictive effect. The full standardized cumulative-logit sensitivity model is reported in Table 6. The restricted observed ranges of vulnerability and impact (both 2–3), together with the concentration of several other ordinal predictors around level 3, further limited the

discrimination available to the regression models. Numerous tied observations and sparsely represented score combinations may reduce statistical power to detect some associations and increase the sensitivity of individual coefficient estimates to a small number of observations. These limitations were compounded by the small number of units in the highest observed STAR risk category (n = 9). Consequently, non-significant associations should not be interpreted as evidence that vulnerability, coping capacity, or other assessment dimensions are substantively unimportant. The regression results remain supplementary descriptions of associations within the restricted observed score distributions rather than estimates of independent causal effects.

Table 5. HC3 regression sensitivity analysis for aggregated risk level (M3).

Predictor	B	95% CI for B	HC3 SE	β	*p*
Probability	0.483	[0.291, 0.675]	0.098	0.479	<0.001
Frequency	0.137	[0.037, 0.238]	0.051	0.176	0.007
Vulnerability	0.347	[0.058, 0.636]	0.147	0.241	0.018
Impact	0.171	[0.032, 0.310]	0.071	0.189	0.016
Exposure	−0.500	[−0.914, −0.085]	0.211	−0.126	0.018
Coping-capacity score	0.149	[−0.050, 0.347]	0.101	0.106	0.143
Hazard count	−0.029	[−0.068, 0.010]	0.020	−0.120	0.139
Data confidence	0.039	[−0.098, 0.176]	0.070	0.038	0.575

Note. N = 161; R^2 = 0.482; adjusted R^2 = 0.455. HC3 robust standard errors and 95% confidence intervals are shown. The model is a sensitivity/decomposition analysis because several predictors are components of STAR impact/risk construction; coefficients must not be interpreted causally—higher coping-capacity score = poorer capacity.

Table 6. Standardized cumulative-logit sensitivity model for higher STAR risk category.

Predictor	Odds Ratio	95% CI	*p*
Probability	5.038	[2.809, 9.036]	<0.001
Frequency	2.168	[1.194, 3.936]	0.011
Vulnerability	2.114	[1.297, 3.445]	0.003
Impact	2.530	[1.284, 4.986]	0.007
Exposure	0.608	[0.317, 1.168]	0.135
Coping-capacity score	1.608	[0.923, 2.804]	0.094
Hazard count	0.620	[0.346, 1.111]	0.108
Data confidence	1.143	[0.658, 1.987]	0.635

Note. Predictors were standardized before estimation. Odds ratios represent the odds of occupying a higher-risk category. These estimates are sensitivity results only because the outcome is algorithmically derived from several STAR components and the high-risk category contains only nine units.

4.6. Exposure-Weighted Portfolio Risk Burden and Aggregation Concordance

The analytical probability-impact product (PIP) had M = 8.18 (SD = 1.70; median = 9; range = 4–12). CHEB, which combines hazard count with the reported unit-level exposure proportion, had M = 2.78 (SD = 1.08), while PRB had M = 22.64 (SD = 10.10). The sample-relative IPDRI therefore had M = 43.64 (SD = 21.45; median = 39.65; range = 0–100). Table 7 summarizes these derived measures nationally, while Supplementary Table S5 provides municipality-level PIP, CHEB, exposure-weighted PIP, PRB, and IPDRI values. We also examined their geographic distributions using GIS-based thematic mapping. Figure 6A,B present CHEB and IPDRI as part of the main spatial results, whereas Supplementary Figures S6–S8 provide municipality-level distributions of PIP, PRB, and exposure-weighted PIP, respectively.

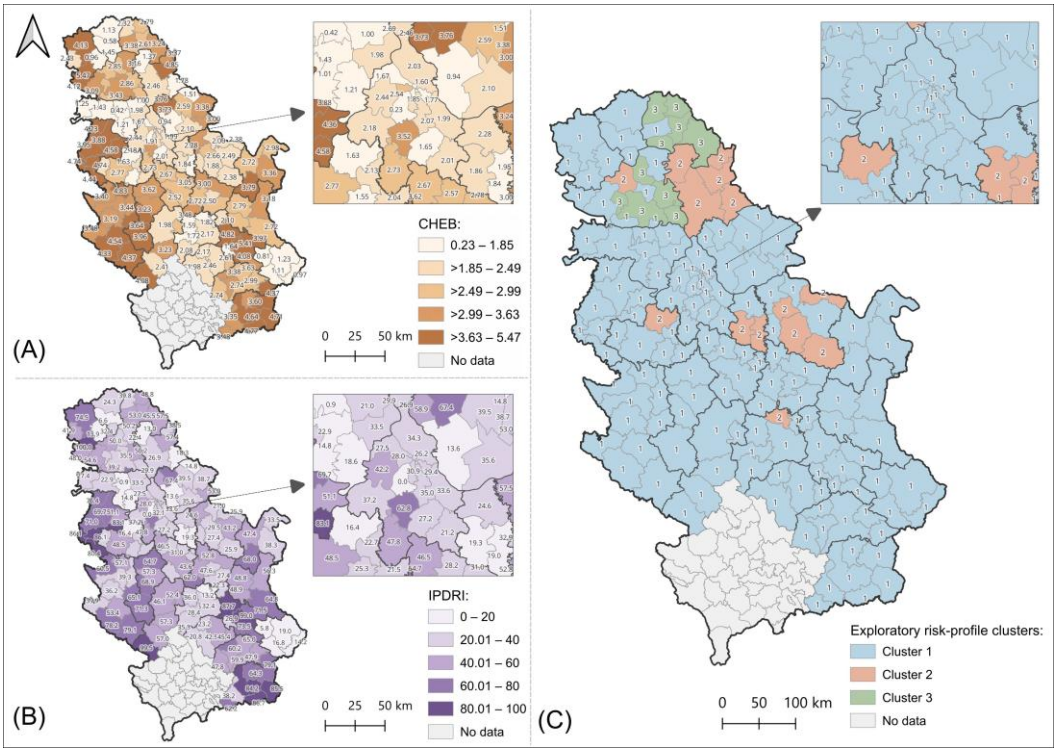


Figure 6. Spatial distribution of complementary portfolio-risk characteristics across Serbian local administrative units: (**A**) cumulative hazard–exposure burden (CHEB); (**B**) Integrated Portfolio Disaster Risk Index (IPDRI); and (**C**) exploratory local risk-profile cluster membership. The inset enlarges the City of Belgrade to preserve the visibility of its 17 city municipalities. IPDRI is a sample-relative 0–100 measure, whereas cluster membership represents an exploratory typology. Areas outside the analytical dataset are shown as No data. Cluster membership represents similarity in assessment attributes rather than geographic clustering. No formal spatial autocorrelation or hotspot analyses were performed.

The strong positive association between CHEB and IPDRI ($r = 0.889$, $p < 0.001$) reflects their shared mathematical construction and should not be interpreted as independent empirical validation. CHEB is a multiplicative component of PRB, while IPDRI is a positive linear transformation of PRB. Although the exact correlation magnitude depends on the observed distribution of the component scores, the association is structurally coupled. By contrast, the weak association between IPDRI and the supplied STAR risk category (Pearson's $r = 0.117$, $p = 0.138$; Spearman's $\varrho = 0.104$, $p = 0.187$) represents a more informative descriptive comparison. This finding indicates limited observed correspondence between the constructed portfolio-burden measure and the supplied categorical assessment, without establishing statistical independence, distinct underlying constructs, or predictive validity. Since CHEB is a multiplicative component of PRB, which is subsequently rescaled to obtain IPDRI, this correlation is partly construction-dependent rather than independent empirical evidence of indicator validity. By contrast, the weak observed association between IPDRI and the supplied STAR risk category ($r = 0.117$, $p = 0.138$) suggests limited correspondence between the constructed portfolio-burden measure and the categorical STAR assessment within this dataset. However, this finding does not establish statistical independence or validate the two measures as distinct underlying constructs.

Table 7. Descriptive characteristics of derived exposure-weighted risk-burden measures.

Measure	Mean	SD	Median	Minimum	Maximum
PIP	8.18	1.70	9.00	4.00	12.00
CHEB	2.78	1.08	2.74	0.23	5.47
Exposure-weighted PIP	2.08	0.96	1.88	0.17	4.45
PRB	22.64	10.10	20.76	2.10	49.19
IPDRI (0–100)	43.64	21.45	39.65	0.00	100.00
Structural susceptibility	2.93	0.21	3.00	2.00	3.50
Hazard dynamics	3.02	0.38	3.00	2.00	4.00

Note. PIP = probability-impact product; CHEB = cumulative hazard-exposure burden; PRB = portfolio risk burden; IPDRI = Integrated Portfolio Disaster Risk Index. IPDRI is a sample-relative rescaling of PRB, not an official WHO STAR score, probability, or expected-loss estimate. The 0–100 IPDRI scale is relative to the observed minimum and maximum PRB values among the 161 administrative units. A value of 0 does not imply zero disaster risk, and a value of 100 does not represent the maximum theoretically possible risk. The index and its quartile-based burden classes are descriptive, sample-dependent measures.

Applying the official STAR risk-matrix thresholds to the aggregate PIP cross-product reproduced the supplied municipality-level STAR risk category in 122 of 161 units (75.8%). Agreement was moderate rather than near-perfect (linear weighted $\kappa = 0.458$; quadratic weighted $\kappa = 0.484$). In 34 units, the PIP-based category was one level lower than the supplied STAR category; in four units, it was one level higher; and in one unit, it was two levels lower. This discrepancy indicates that the cross-product of supplied unit-level probability and impact scores does not fully reproduce the reported STAR categories, although its underlying causes cannot be established without hazard-level data and documented aggregation procedures.

The constructed IPDRI showed a weak and non-significant association with the supplied ordinal STAR risk category (Spearman's $\varrho = 0.104$, $p = 0.187$; Kendall's τ-b = 0.084). In supplementary Pearson analyses of derived measures, IPDRI was moderately correlated with PIP ($r = 0.394$, $p < 0.001$) and strongly correlated with CHEB ($r = 0.889$, $p < 0.001$). These latter associations were interpreted cautiously because the indices share mathematical components. The quartile-based IPDRI burden class was also not significantly associated with the supplied STAR risk category, $\chi^2(6) = 7.21$, $p = 0.302$, bias-corrected Cramér's V = 0.061. Together, these findings indicated limited observed correspondence between the constructed portfolio-burden measure and the categorical STAR risk assessment, without establishing their statistical independence or independent construct validity.

4.7. Macroregional and District-Level Differences in Portfolio Burden

IPDRI differed across the three macroregional groupings, Welch $F(2, 53.15) = 10.11$, $p < 0.001$. Mean IPDRI was highest in Central Serbia (M = 48.31, SD = 22.09), followed by Vojvodina (M = 37.75, SD = 19.76) and Belgrade (M = 32.00, SD = 12.74). Vojvodina had a lower mean than Central Serbia, Welch $t(94.47) = -2.86$, $p = 0.005$, Hedges' $g = -0.49$, and Belgrade had a lower burden than all other units combined, Welch $t(28.69) = -3.63$, $p = 0.001$, $g = -0.61$. At the 25-district level, IPDRI heterogeneity was pronounced: classical $F(24, 136) = 7.65$, $p < 0.001$, $\eta^2 = 0.574$; Welch $F(24, 38.79) = 14.12$, $p < 0.001$; and Kruskal–Wallis $H(24) = 93.55$, $p < 0.001$, $\varepsilon^2 = 0.511$. The highest district-level mean IPDRI values occurred in Mačva (M = 75.49), Pčinja (M = 70.39), and Moravica (M = 65.56), whereas the lowest means occurred in Pirot (M = 13.97), Srem (M = 19.87), and the Danube district (M = 20.98). Table 8 summarizes macroregional descriptive statistics for IPDRI and PRB. Full

district rankings and Holm-adjusted pairwise contrasts are provided in the supplementary workbook.

These macroregional differences should be interpreted with caution because the Belgrade group comprises 17 city municipalities, whereas the comparison groups consist of other local self-government units operating within different administrative and territorial contexts. Consequently, the lower observed IPDRI in Belgrade cannot be attributed exclusively to differences in underlying hazard exposure or risk characteristics. Administrative scale, population distribution, reporting practices, and institutional arrangements may also contribute to these contrasts. The comparisons therefore represent descriptive differences between the observed administrative groups rather than scale-adjusted estimates of underlying risk.

Table 8. Macroregional distribution of exposure-weighted portfolio burden.

Macroregion	n	IPDRI Mean	IPDRI SD	PRB Mean	PRB SD
Belgrade	17	32.00	12.74	17.16	6.00
Vojvodina	45	37.75	19.76	19.87	9.31
Central Serbia	99	48.31	22.09	24.85	10.40

Note. IPDRI = Integrated Portfolio Disaster Risk Index; PRB = portfolio risk burden. Macroregional classification was used as a complementary descriptive grouping and does not replace the 25-district analysis.

Exploratory K-means clustering based on standardized frequency, CHEB, vulnerability, and coping-capacity scores identified three local assessment profiles (n = 137, 14, and 10; silhouette = 0.549). Descriptive comparisons indicated differences in the supplied STAR risk category and PIP across these groups. However, these comparisons did not constitute external validation because the grouping variables and the comparison measures originated from the same assessment system and shared direct or indirect construction pathways. The cluster characteristics and corresponding statistical comparisons are presented in Section 4.12. The IPDRI distribution was broad rather than concentrated around a single category, indicating substantial heterogeneity in exposure-weighted portfolio burden even though the official STAR risk category was predominantly moderate. This contrast supports treating categorical risk intensity and cumulative portfolio burden as analytically distinct dimensions, while the corresponding macroregional distribution of IPDRI.

4.8. Extended Risk-Group Profiles and Model Diagnostics

To characterize how component scores change across the three observed STAR risk categories, we compared each raw variable across low, moderate, and high risk groups. Probability displayed the largest separation ($\varepsilon^2 = 0.307$), followed by frequency ($\varepsilon^2 = 0.128$), vulnerability ($\varepsilon^2 = 0.087$), impact ($\varepsilon^2 = 0.062$), and coping-capacity score ($\varepsilon^2 = 0.046$). Hazard count, exposure, and data confidence did not differ significantly after Holm correction. These comparisons are descriptive because the STAR risk algorithm embeds probability and impact, while frequency informs probability and vulnerability/coping capacity inform impact (Table 9).

Table 9. STAR component profiles across low, moderate, and high risk categories.

Variable	Low Median (IQR)	Moderate Median (IQR)	High Median (IQR)	H	Holm *p*	ε^2
Hazard count	10.000 (10.000–11.750)	10.000 (10.000–12.000)	11.000 (10.000–11.000)	0.40	0.818	0.000

Variable	Low Median (IQR)	Moderate Median (IQR)	High Median (IQR)	H	Holm *p*	ε^2
Exposure proportion	0.289 (0.246–0.313)	0.258 (0.183–0.325)	0.180 (0.122–0.298)	3.19	0.610	0.008
Frequency score	3.000 (2.000–3.000)	3.000 (3.000–3.000)	4.000 (3.000–4.000)	22.28	<0.001	0.128
Probability score	3.000 (2.000–3.000)	3.000 (3.000–3.000)	4.000 (4.000–4.000)	50.51	<0.001	0.307
Impact score	2.000 (2.000–3.000)	3.000 (3.000–3.000)	3.000 (3.000–3.000)	11.76	0.014	0.062
Coping-capacity score (higher = poorer capacity)	3.000 (3.000–3.000)	3.000 (3.000–3.000)	3.000 (3.000–3.000)	9.28	0.039	0.046
Vulnerability score	3.000 (2.000–3.000)	3.000 (3.000–3.000)	3.000 (3.000–3.000)	15.77	0.002	0.087
Data confidence score	2.000 (2.000–2.000)	2.000 (2.000–2.000)	2.000 (2.000–2.000)	2.44	0.610	0.003

Note. Low, moderate, and high correspond to STAR risk categories 2, 3, and 4. Higher coping-capacity scores indicate poorer coping capacity. Omnibus tests are Kruskal–Wallis tests.

The OLS sensitivity model showed no material multicollinearity or evidence of heteroskedasticity, but residuals were not normally distributed. Influence diagnostics identified a subset of observations with elevated Cook's distance or leverage, while the model remained stable in the influence sensitivity analysis. These findings support using HC3 robust errors and the primacy of ordinal/nonparametric analyses (Table 10).

Table 10. Diagnostic and robustness checks for the model-based sensitivity analyses.

Diagnostic	Result	Interpretation
M3 VIF range	1.13–1.31	No material multicollinearity.
Breusch–Pagan	LM = 8.505, $p = 0.386$	No evidence of heteroskedasticity.
White test	LM = 35.884, $p = 0.656$	No evidence of heteroskedasticity.
Jarque–Bera	JB = 45.649, $p < 0.001$	Residuals are non-normal.
Shapiro–Wilk	W = 0.939, $p < 0.001$	Residuals are non-normal; HC3 and ordinal/nonparametric analyses are preferred.
Ramsey RESET	F = 0.064, $p = 0.801$	No evidence of simple functional-form misspecification.
Cook's distance	20 cases > 4/N; max = 0.107	Influence exists; sensitivity analysis was run.
High leverage	17 cases > 2(k + 1)/N; max = 0.201	Some leverage expected from sparse ordinal patterns.
District × risk	Chi-square = 150.199, df = 48; asymptotic $p <$ 0.001; Monte Carlo $p = 0.0002$; bias-corrected Cramer's V = 0.566	Strong regional association; Monte Carlo inference used because many expected counts are <5.
Risk one-way ANOVA sensitivity	F(24,136) = 5.959, $p < 0.001$, eta2 = 0.513, omega2 = 0.425	Large regional effect; primary test remains Kruskal–Wallis because the outcome is ordinal.
Brown–Forsythe sensitivity	F* = 5.415, $p = 0.00005$	Regional difference remains under robust variance correction.

4.9. Derived-Variable Correlations and Two-Group Comparisons

The derived-variable analysis examined associations between the constructed portfolio-burden measures and the supplied WHO STAR assessment indicators, prioritizing rank-based correlations whenever ordinal variables were involved. IPDRI showed a weak and statistically non-significant association with the supplied STAR risk category (Spearman's $\rho = 0.104$, $p = 0.187$; Kendall's τ-b = 0.084), whereas PIP demonstrated a moderate positive association with STAR risk ($\rho = 0.522$, $p < 0.001$). PIP was also positively associated with impact ($\rho = 0.812$, $p < 0.001$) and probability ($\rho = 0.477$, $p < 0.001$), while IPDRI showed positive associations with impact ($\rho = 0.409$, $p < 0.001$) and vulnerability ($\rho = 0.263$, $p < 0.001$). For sufficiently continuous measures, supplementary Pearson correlations indicated strong positive associations between IPDRI and exposure

(r = 0.835, 95% CI [0.781, 0.877], $p < 0.001$), CHEB and exposure (r = 0.940, $p < 0.001$), and CHEB and IPDRI (r = 0.889, 95% CI [0.852, 0.918], $p < 0.001$). Consequently, their statistical significance does not independently establish indicator validity, predictive performance, or operational usefulness. These strong correlations are construction-dependent because exposure contributes to CHEB, CHEB is a component of PRB, and IPDRI is a positive linear rescaling of PRB. Therefore, the associations primarily reflect shared algebraic components rather than independent evidence of index validity, although their exact magnitudes depend on the observed data. The weak and statistically non-significant IPDRI–STAR association represents the more informative descriptive contrast, but it does not establish statistical independence, incremental predictive performance, or validity as a distinct risk construct. Table 11 presents selected Pearson correlations as supplementary descriptive estimates to facilitate comparison with the original analyses, while Supplementary Table S1 provides the complete Pearson and Spearman correlation results. Associations involving ordinal STAR indicators were primarily interpreted using Spearman's ϱ, with Kendall's τ-b serving as a sensitivity measure to account for tied observations. Pearson correlations involving ordinal indicators were retained for descriptive completeness rather than as the primary basis for statistical interpretation. Furthermore, correlations among mathematically related derived measures were interpreted cautiously because of their shared construction components.

Table 11. Selected Pearson correlations for the derived risk-burden measures.

Derived Measure	Reference Variable	r	95% CI	*p*	Holm *p*
PIP	probability	0.582	[0.470, 0.676]	<0.001	<0.001
PIP	impact	0.754	[0.679, 0.814]	<0.001	<0.001
PIP	vulnerability	0.333	[0.188, 0.464]	<0.001	<0.001
PIP	star_risk	0.567	[0.452, 0.664]	<0.001	<0.001
CHEB	exposure	0.940	[0.919, 0.956]	<0.001	<0.001
CHEB	star_risk	−0.150	[−0.298, 0.005]	0.058	0.462
PRB	exposure	0.835	[0.781, 0.877]	<0.001	<0.001
PRB	star_risk	0.117	[−0.038, 0.267]	0.138	0.555
IPDRI	exposure	0.835	[0.781, 0.877]	<0.001	<0.001
IPDRI	impact	0.389	[0.250, 0.513]	<0.001	<0.001
IPDRI	vulnerability	0.232	[0.080, 0.373]	0.003	0.022
IPDRI	star_risk	0.117	[−0.038, 0.267]	0.138	0.555

Note. The complete 63-row Pearson/Spearman matrix is provided in Supplementary Table S1.

Welch tests identified several substantively meaningful contrasts. Belgrade had lower IPDRI than all other units (M = 32.00 vs. 45.01), t(28.69) = −3.63, $p = 0.001$, g = −0.61, and lower CHEB, t(27.35) = −4.73, $p < 0.001$, g = −0.83. Vojvodina also had lower IPDRI than Central Serbia (M = 37.75 vs. 48.31), t(94.47) = −2.86, $p = 0.005$, g = −0.49. Units with data-confidence score 3 showed lower structural susceptibility than units with score 2, t(38.15) = −3.28, $p = 0.002$, g = −0.79. Mann–Whitney sensitivity tests generally supported the principal regional burden contrasts. Table 12 summarizes the complete set of statistically significant pre-specified comparisons and shows the distribution of the aggregated PIP across the supplied STAR risk categories.

Table 12. Statistically significant Welch independent-samples comparisons and nonparametric sensitivity tests.

Comparison	Variable	Group 1 n/M	Group 2 n/M	t (df)	*p*	Hedges g	MW *p*
Data confidence: score 3 vs. score 2	struct_susc	31/2.81	130/2.96	−3.28 (38.15)	0.002	−0.79	<0.001
Belgrade vs. all other units	IPDRI	17/32.00	144/45.01	−3.63 (28.69)	0.001	−0.61	0.023
Belgrade vs. all other units	CHEB	17/2.00	144/2.87	−4.73 (27.35)	<0.001	−0.83	<0.001
Belgrade vs. all other units	PRB	17/17.16	144/23.29	−3.63 (28.69)	0.001	−0.61	0.023
Belgrade vs. all other units	struct_susc	17/3.00	144/2.92	4.25 (143.00)	<0.001	0.37	0.131
Vojvodina vs. Central Serbia	IPDRI	45/37.75	99/48.31	−2.86 (94.47)	0.005	−0.49	0.011
Vojvodina vs. Central Serbia	CHEB	45/2.53	99/3.02	−2.44 (76.93)	0.017	−0.46	0.030
Vojvodina vs. Central Serbia	PRB	45/19.87	99/24.85	−2.86 (94.47)	0.005	−0.49	0.011
Vojvodina vs. Central Serbia	struct_susc	45/2.82	99/2.97	−3.25 (56.45)	0.002	−0.71	<0.001
Vojvodina vs. Central Serbia	star_risk	45/2.80	99/3.00	−2.25 (60.90)	0.028	−0.47	0.008

Note. The full set of 18 pre-specified Welch tests is reproduced in Supplementary Table S2. Belgrade-versus-other comparisons are potentially confounded by differences in administrative scale, population structure, and institutional organization. The reported estimates were not adjusted for territorial area or population size.

4.10. Parametric and Robust Macroregional and District-Level Comparisons

Macroregional comparisons demonstrated that the strongest differences involved exposure-related burden rather than PIP itself. CHEB, exposure-weighted PIP, PRB, IPDRI, and structural susceptibility differed across macroregions. For IPDRI, classical ANOVA yielded $F(2, 158) = 7.04$, $p = 0.001$, $\eta^2 = 0.082$; Welch ANOVA was also significant, $F(2, 53.15) = 10.11$, $p < 0.001$, and the Kruskal–Wallis sensitivity test remained significant, $H = 11.59$, $p = 0.003$, $\varepsilon^2 = 0.061$. PIP and hazard dynamics did not differ materially across macroregions. Table 13 reports the complete macroregional omnibus results, and Table 14 reports the significant Holm-adjusted pairwise contrasts. Supplementary Figures S9 and S10 show the municipality-level spatial distributions of structural susceptibility and hazard dynamics, respectively.

Table 13. Macroregional comparisons using Welch ANOVA and Kruskal–Wallis tests.

Variable	Welch F	Welch *p*	H	KW *p*	ε^2
Star_Risk	—	—	8.24	0.016	0.040
PIP	1.69	0.195	2.27	0.321	0.002
CHEB	14.70	<0.001	16.47	<0.001	0.092
EW_PIP	14.32	<0.001	14.23	<0.001	0.077
PRB	10.11	<0.001	11.59	0.003	0.061
IPDRI	10.11	<0.001	11.59	0.003	0.061
Struct_Susc	—	—	18.22	<0.001	0.103
Hazard_Dynamics	—	—	0.42	0.812	−0.010

Note. Welch statistics are omitted where zero within-group variance prevented stable estimation.

Table 14. Significant Holm-adjusted macroregional pairwise contrasts.

Variable	Comparison	Means	Welch t (df)	Holm *p*	Hedges g
CHEB	Belgrade vs. Vojvodina	2.00 vs. 2.53	−2.29 (49.61)	0.034	−0.51
CHEB	Belgrade vs. Central Serbia	2.00 vs. 3.02	−5.37 (30.87)	<0.001	−1.04
CHEB	Vojvodina vs. Central Serbia	2.53 vs. 3.02	−2.44 (76.93)	0.034	−0.46
EW_PIP	Belgrade vs. Vojvodina	1.46 vs. 1.82	−2.03 (44.97)	0.048	−0.47
EW_PIP	Belgrade vs. Central Serbia	1.46 vs. 2.31	−5.26 (40.85)	<0.001	−0.88

Variable	Comparison	Means	Welch t (df)	Holm *p*	Hedges g
EW_PIP	Vojvodina vs. Central Serbia	1.82 vs. 2.31	−3.16 (105.15)	0.004	−0.52
PRB	Belgrade vs. Central Serbia	17.16 vs. 24.85	−4.29 (35.24)	<0.001	−0.77
PRB	Vojvodina vs. Central Serbia	19.87 vs. 24.85	−2.86 (94.47)	0.010	−0.49
IPDRI	Belgrade vs. Central Serbia	32.00 vs. 48.31	−4.29 (35.24)	<0.001	−0.77
IPDRI	Vojvodina vs. Central Serbia	37.75 vs. 48.31	−2.86 (94.47)	0.010	−0.49
struct_susc	Belgrade vs. Vojvodina	3.00 vs. 2.82	4.18 (44.00)	<0.001	0.72
struct_susc	Vojvodina vs. Central Serbia	2.82 vs. 2.97	−3.25 (56.45)	0.004	−0.71

Note. All 24 macroregional pairwise estimates are provided in Supplementary Table S3. Large Hedges' g values should be interpreted cautiously where within-group variability is restricted, and raw mean differences should be prioritized when evaluating substantive magnitude.

District-level heterogeneity was substantially larger than macroregional heterogeneity. CHEB showed the largest district effect (classical $\eta^2 = 0.644$; Kruskal–Wallis $\varepsilon^2 = 0.607$), followed by exposure-weighted PIP ($\eta^2 = 0.631$; $\varepsilon^2 = 0.555$), PRB/IPDRI ($\eta^2 = 0.574$; $\varepsilon^2 = 0.511$), and PIP ($\eta^2 = 0.413$; $\varepsilon^2 = 0.290$). IPDRI remained highly heterogeneous under Welch ANOVA, $F(24, 38.79) = 14.12$, $p < 0.001$. Tables 15 and 16 summarize the district-level omnibus results for the derived burden measures and the corresponding Holm-significant pairwise contrasts for IPDRI, CHEB, and PIP, respectively.

Table 15. District-level comparisons using Welch ANOVA and Kruskal–Wallis tests.

Variable	Welch F	Welch *p*	H	KW *p*	ε^2
PIP	—	—	63.48	<0.001	0.290
CHEB	26.86	<0.001	106.61	<0.001	0.607
EW_PIP	18.12	<0.001	99.54	<0.001	0.555
PRB	14.12	<0.001	93.55	<0.001	0.511
IPDRI	14.12	<0.001	93.55	<0.001	0.511

Table 16. Holm-significant district pairwise contrasts for IPDRI, CHEB, and PIP.

Variable	District Comparison	Means	Welch t (df)	Holm *p*	Hedges g
IPDRI	Grad Beograd vs. Moravički	32.00 vs. 65.56	−7.70 (10.17)	0.004	−2.70
IPDRI	Grad Beograd vs. Mačvanski	32.00 vs. 75.49	−8.43 (14.98)	<0.001	−3.38
IPDRI	Šumadijski vs. Moravički	35.24 vs. 65.56	−7.47 (7.14)	0.035	−4.11
IPDRI	Šumadijski vs. Mačvanski	35.24 vs. 75.49	−8.20 (11.65)	0.001	−3.86
IPDRI	Južno-Bački vs. Pirotski	41.32 vs. 13.97	5.62 (12.57)	0.026	2.10
IPDRI	Južno-Bački vs. Mačvanski	41.32 vs. 75.49	−6.01 (16.66)	0.004	−2.54
IPDRI	Moravički vs. Rasinski	65.56 vs. 27.33	7.78 (7.99)	0.015	4.15
IPDRI	Moravički vs. Pirotski	65.56 vs. 13.97	12.23 (5.98)	0.005	7.52
IPDRI	Moravički vs. Braničevski	65.56 vs. 32.91	6.27 (9.89)	0.027	2.87
IPDRI	Moravički vs. Podunavski	65.56 vs. 20.98	12.45 (4.63)	0.027	7.26
IPDRI	Moravički vs. Sremski	65.56 vs. 19.87	9.19 (8.90)	0.002	4.56
IPDRI	Severno-Banatski vs. Pirotski	49.14 vs. 13.97	9.22 (6.85)	0.012	5.31
IPDRI	Severno-Banatski vs. Podunavski	49.14 vs. 20.98	9.10 (6.85)	0.013	4.61
IPDRI	Severno-Banatski vs. Sremski	49.14 vs. 19.87	6.32 (9.90)	0.025	3.14
IPDRI	Rasinski vs. Mačvanski	27.33 vs. 75.49	−8.55 (11.90)	<0.001	−4.18
IPDRI	Jablanički vs. Pirotski	57.94 vs. 13.97	7.88 (7.62)	0.018	4.01
IPDRI	Jablanički vs. Sremski	57.94 vs. 19.87	6.17 (10.14)	0.027	3.23
IPDRI	Pirotski vs. Mačvanski	13.97 vs. 75.49	−12.21 (9.96)	<0.001	−5.53
IPDRI	Pirotski vs. Zlatiborski	13.97 vs. 54.86	−7.00 (12.00)	0.004	−2.69
IPDRI	Pirotski vs. Pčinjski	13.97 vs. 70.39	−7.84 (7.94)	0.015	−3.52
IPDRI	Braničevski vs. Mačvanski	32.91 vs. 75.49	−7.22 (14.00)	0.001	−3.41

IPDRI	Podunavski vs. Mačvanski	20.98 vs. 75.49	−12.06 (8.83)	<0.001	−4.79
IPDRI	Podunavski vs. Zlatiborski	20.98 vs. 54.86	−6.28 (10.68)	0.019	−2.16
IPDRI	Mačvanski vs. Sremski	75.49 vs. 19.87	9.78 (12.99)	<0.001	4.72
IPDRI	Mačvanski vs. Kolubarski	75.49 vs. 28.52	7.36 (10.80)	0.005	3.73
IPDRI	Sremski vs. Zlatiborski	19.87 vs. 54.86	−5.46 (14.95)	0.019	−2.36
IPDRI	Sremski vs. Pčinjski	19.87 vs. 70.39	−6.59 (9.75)	0.019	−3.30
CHEB	Grad Beograd vs. Južno-Bački	2.00 vs. 3.13	−5.67 (26.66)	0.001	−1.92
CHEB	Grad Beograd vs. Moravički	2.00 vs. 3.66	−7.33 (10.09)	0.007	−2.57
CHEB	Grad Beograd vs. Pirotski	2.00 vs. 1.03	5.23 (18.03)	0.015	1.51
CHEB	Grad Beograd vs. Mačvanski	2.00 vs. 4.36	−11.93 (22.82)	<0.001	−3.94
CHEB	Grad Beograd vs. Zlatiborski	2.00 vs. 3.87	−7.64 (20.99)	<0.001	−2.85
CHEB	Grad Beograd vs. Pčinjski	2.00 vs. 4.08	−7.31 (11.96)	0.003	−3.08
CHEB	Šumadijski vs. Rasinski	2.75 vs. 1.79	6.86 (8.02)	0.033	3.69
CHEB	Šumadijski vs. Pirotski	2.75 vs. 1.03	15.07 (6.34)	<0.001	8.65
CHEB	Šumadijski vs. Mačvanski	2.75 vs. 4.36	−11.98 (11.11)	<0.001	−5.62
CHEB	Šumadijski vs. Sremski	2.75 vs. 1.19	8.10 (7.70)	0.013	4.05
CHEB	Šumadijski vs. Zlatiborski	2.75 vs. 3.87	−5.69 (11.31)	0.032	−2.28
CHEB	Toplički vs. Mačvanski	2.30 vs. 4.36	−11.23 (7.05)	0.003	−6.01
CHEB	Toplički vs. Zlatiborski	2.30 vs. 3.87	−6.71 (11.15)	0.008	−2.78
CHEB	Toplički vs. Pčinjski	2.30 vs. 4.08	−6.46 (8.82)	0.032	−3.04
CHEB	Južno-Bački vs. Rasinski	3.13 vs. 1.79	7.89 (13.53)	<0.001	3.36
CHEB	Južno-Bački vs. Pirotski	3.13 vs. 1.03	14.04 (12.23)	<0.001	5.31
CHEB	Južno-Bački vs. Mačvanski	3.13 vs. 4.36	−7.44 (17.23)	<0.001	−3.11
CHEB	Južno-Bački vs. Sremski	3.13 vs. 1.19	9.02 (11.18)	<0.001	4.27
CHEB	Moravički vs. Rasinski	3.66 vs. 1.79	9.29 (6.17)	0.019	5.52
CHEB	Moravički vs. Pirotski	3.66 vs. 1.03	14.24 (4.74)	0.012	8.76
CHEB	Moravički vs. Sremski	3.66 vs. 1.19	10.26 (8.53)	0.001	5.26
CHEB	Moravički vs. Kolubarski	3.66 vs. 2.05	6.72 (7.82)	0.041	3.67
CHEB	Severno-Banatski vs. Pirotski	2.87 vs. 1.03	9.91 (7.43)	0.004	5.00
CHEB	Severno-Banatski vs. Mačvanski	2.87 vs. 4.36	−7.53 (9.70)	0.006	−3.91
CHEB	Severno-Banatski vs. Sremski	2.87 vs. 1.19	6.96 (11.00)	0.007	3.54
CHEB	Rasinski vs. Mačvanski	1.79 vs. 4.36	−15.31 (11.51)	<0.001	−7.61
CHEB	Rasinski vs. Zaječarski	1.79 vs. 2.87	−6.71 (7.89)	0.040	−3.64
CHEB	Rasinski vs. Zlatiborski	1.79 vs. 3.87	−9.39 (13.80)	<0.001	−3.91
CHEB	Rasinski vs. Pčinjski	1.79 vs. 4.08	−8.65 (8.86)	0.004	−4.25
CHEB	Jablanički vs. Pirotski	3.26 vs. 1.03	8.39 (6.23)	0.032	4.06
CHEB	Jablanički vs. Sremski	3.26 vs. 1.19	6.75 (9.42)	0.017	3.57
CHEB	Pirotski vs. Pomoravski	1.03 vs. 2.90	−7.77 (6.50)	0.040	−3.79
CHEB	Pirotski vs. Braničevski	1.03 vs. 2.37	−7.33 (9.87)	0.007	−3.19
CHEB	Pirotski vs. Mačvanski	1.03 vs. 4.36	−22.55 (9.72)	<0.001	−10.49
CHEB	Pirotski vs. Zaječarski	1.03 vs. 2.87	−13.21 (5.87)	0.004	−8.12
CHEB	Pirotski vs. Zlatiborski	1.03 vs. 3.87	−13.76 (11.81)	<0.001	−5.16
CHEB	Pirotski vs. Pčinjski	1.03 vs. 4.08	−12.09 (7.59)	<0.001	−5.38
CHEB	Pomoravski vs. Sremski	2.90 vs. 1.19	5.99 (10.08)	0.033	3.13
CHEB	Braničevski vs. Mačvanski	2.37 vs. 4.36	−10.11 (12.85)	<0.001	−4.78
CHEB	Braničevski vs. Zlatiborski	2.37 vs. 3.87	−6.13 (15.99)	0.004	−2.69
CHEB	Braničevski vs. Pčinjski	2.37 vs. 4.08	−6.01 (10.81)	0.024	−2.99
CHEB	Podunavski vs. Mačvanski	2.00 vs. 4.36	−12.79 (4.88)	0.016	−6.90
CHEB	Podunavski vs. Zlatiborski	2.00 vs. 3.87	−7.99 (8.75)	0.007	−3.23
CHEB	Podunavski vs. Pčinjski	2.00 vs. 4.08	−7.55 (7.98)	0.017	−3.40
CHEB	Mačvanski vs. Sremski	4.36 vs. 1.19	14.83 (10.50)	<0.001	7.41
CHEB	Mačvanski vs. Zaječarski	4.36 vs. 2.87	9.52 (9.03)	0.001	4.62
CHEB	Mačvanski vs. Kolubarski	4.36 vs. 2.05	10.87 (9.01)	<0.001	5.74

CHEB	Sremski vs. Zaječarski	1.19 vs. 2.87	−8.07 (8.76)	0.007	−3.78
CHEB	Sremski vs. Zlatiborski	1.19 vs. 3.87	−10.39 (14.55)	<0.001	−4.68
CHEB	Sremski vs. Pčinjski	1.19 vs. 4.08	−9.77 (11.24)	<0.001	−4.89
CHEB	Severno-Bački vs. Pčinjski	1.05 vs. 4.08	−8.74 (5.52)	0.048	−4.70
CHEB	Zlatiborski vs. Kolubarski	3.87 vs. 2.05	7.08 (13.11)	0.002	3.21
CHEB	Kolubarski vs. Pčinjski	2.05 vs. 4.08	−6.88 (10.66)	0.008	−3.46
PIP	Grad Beograd vs. Podunavski	8.65 vs. 6.00	10.95 (16.00)	<0.001	2.70
PIP	Grad Beograd vs. Srednje-Banatski	8.65 vs. 6.00	10.95 (16.00)	<0.001	2.86
PIP	Moravički vs. Podunavski	9.00 vs. 6.00	— (—)	<0.001	—
PIP	Moravički vs. Srednje-Banatski	9.00 vs. 6.00	— (—)	<0.001	—
PIP	Severno-Banatski vs. Podunavski	8.83 vs. 6.00	17.00 (5.00)	0.004	7.30
PIP	Severno-Banatski vs. Srednje-Banatski	8.83 vs. 6.00	17.00 (5.00)	0.004	8.51
PIP	Jablanički vs. Podunavski	9.00 vs. 6.00	— (—)	<0.001	—
PIP	Jablanički vs. Srednje-Banatski	9.00 vs. 6.00	— (—)	<0.001	—
PIP	Podunavski vs. Zapadno-Bački	6.00 vs. 9.00	— (—)	<0.001	—
PIP	Zapadno-Bački vs. Srednje-Banatski	9.00 vs. 6.00	— (—)	<0.001	—

Note. Ninety Holm-significant contrasts are shown. The accompanying statistical workbook includes all 900 pairwise estimates, including non-significant comparisons. Hedges' g values may be inflated or unstable when pooled within-group variability is very small. Comparisons for which both groups have zero within-group variance are not considered estimable by conventional Welch tests and should not be assigned Welch-derived significance levels. Raw differences should be interpreted alongside the variability and sample size of the compared groups.

4.11. Complementary Sensitivity Models and Aggregation Concordance

As an additional sensitivity analysis, complementary regression models were estimated to examine associations between the constructed probability–impact product (PIP), cumulative hazard–exposure burden (CHEB), and selected assessment characteristics while excluding direct score-construction components from the predictor set. These models were intended to assess the sensitivity of the descriptive relationships to alternative model specifications rather than establish statistical independence, causal mechanisms, or external validation. The corresponding regression results were therefore interpreted as exploratory sensitivity findings.

To separate exposure burden from STAR's formative probability–impact algorithm, we regressed PIP only on CHEB, data confidence, and macroregion. The HC3 model was not significant (R^2 = 0.012, adjusted R^2 = −0.014, model p = 0.406), and none of the non-constitutive predictors were associated with PIP (Table 17). This finding indicates limited explanatory power but does not establish statistical independence between the two measures.

Table 17. Non-circular HC3 regression model for the analytical probability–impact product.

Predictor	B	HC3 SE	95% CI	*p*
Intercept	8.699	0.966	[6.806, 10.593]	<0.001
CHEB	−0.034	0.137	[−0.302, 0.235]	0.806
Data confidence	−0.212	0.349	[−0.896, 0.472]	0.544
Vojvodina vs. Central Serbia	−0.028	0.349	[−0.711, 0.656]	0.937

Note. N = 161; R^2 = 0.012; adjusted R^2 = −0.014; model p = 0.406. We excluded probability, impact, vulnerability, and coping capacity from the predictor set to avoid direct mathematical coupling.

In the exploratory non-circular ordered-logit model, higher CHEB was associated with lower odds of occupying a higher supplied STAR risk category (OR = 0.586, 95% CI

[0.380, 0.902], $p = 0.015$). Vojvodina had lower odds than Central Serbia (OR = 0.200, 95% CI [0.073, 0.543], $p = 0.002$). Data confidence and the Belgrade indicator were not significant. Because only categories 2–4 were observed and we assumed a proportional-odds structure, we interpret this model as exploratory. The full exploratory ordered-logit estimates are reported in Table 18.

Table 18. Exploratory non-circular ordered-logit model for the supplied STAR risk category.

Predictor	B	SE	*p*	Odds Ratio	95% CI OR
CHEB	−0.535	0.220	0.015	0.586	[0.380, 0.902]
Data confidence	−0.389	0.551	0.480	0.678	[0.230, 1.994]
Vojvodina vs. Central Serbia	−1.610	0.510	0.002	0.200	[0.073, 0.543]
Belgrade vs. Central Serbia	−0.629	0.801	0.432	0.533	[0.111, 2.561]

Applying the official STAR matrix thresholds to the aggregate PIP cross-product reproduced the supplied risk category in 122 units (75.8%) and disagreed in 39 units. Weighted agreement was moderate (linear $\kappa = 0.458$; quadratic $\kappa = 0.484$). The discrepancy demonstrates that aggregating probability and impact before applying the risk matrix is not equivalent to aggregating hazard-specific risk results. Table 19 summarizes agreement metrics and the cross-classification of the two risk categorizations.

Table 19. Agreement between the PIP-derived risk-matrix category and the supplied STAR risk category.

Agreement Metric	Value
Exact agreement	75.8%
Disagreement	39 units
Weighted κ (linear)	0.458
Weighted κ (quadratic)	0.484

Quartile-based IPDRI burden class was not significantly associated with the supplied STAR risk category, $\chi^2(6) = 7.21$, $p = 0.302$, bias-corrected Cramér's V = 0.061. This weak cross-classification is consistent with the correlation results and supports interpretation of IPDRI as a complementary portfolio/exposure burden dimension rather than a replacement for STAR risk intensity.

The index-construction sensitivity analysis showed that baseline PRB rankings were sensitive to alternative specifications. Spearman correlations ranged from 0.780 to 0.983, with 12–18 of the baseline top 20 administrative units retained. The intensity-weighted alternative (75:25) produced the greatest ranking changes ($\varrho = 0.780$; 12/20 overlap). A monotonic logarithmic transformation preserved the baseline rankings by construction and was not interpreted as evidence of substantive robustness. These findings demonstrate specification sensitivity rather than establish an optimal weighting scheme or independent index validity.

4.12. Exploratory Risk-Profile Clustering and Sensitivity Analysis

Exploratory K-means clustering of standardized frequency, CHEB, vulnerability, and coping-capacity scores identified a three-cluster solution with the highest silhouette coefficient among the examined k = 2–6 alternatives (silhouette = 0.5485). The resulting partition comprised 137, 14, and 10 local administrative units. Thus, the dominant cluster included 85.1% of all administrative units, whereas the two smaller clusters accounted for

8.7% and 6.2%, respectively. This pronounced asymmetry limits the typology's ability to distinguish preparedness profiles among most administrative units and warrants cautious operational interpretation. An internal reproducibility check based on the rounded values reported in Supplementary Tables S5 and S6 reproduced the reported cluster membership exactly, up to cluster-label permutation (ARI = 1.000). Moreover, a three-cluster hierarchical solution obtained using Ward's linkage yielded the same partition (ARI = 1.000). These findings indicated consistency across the two clustering algorithms under the specified input conditions. However, they did not establish that the identified profiles represent natural, externally validated, or operationally distinct risk types. The interpretation remains exploratory because several clustering inputs are ordinal, the clusters are highly unequal in size, and the sensitivity checks were based on rounded assessment values. The cluster characteristics and corresponding statistical comparisons are presented in Section 4.12 and Table 20.

Table 20. Profiles of the three exploratory local risk clusters.

Cluster	n	Frequency	CHEB	Vulnerability	Coping-Capacity Score	Probability	Impact	STAR Risk	PIP	IPDRI
1	137	3.06	2.81	3.00	3.02	3.03	2.78	3.01	8.41	45.45
2	14	3.00	2.37	2.00	2.93	3.07	2.07	2.57	6.36	27.58
3	10	2.80	2.86	3.00	2.00	2.70	2.80	2.60	7.60	41.34

Note. Higher coping-capacity scores indicate poorer coping capacity. The table reports original STAR scores, whereas K-means clustering used standardized frequency, CHEB, vulnerability, and coping-capacity scores.

The cluster stability analysis revealed different levels of robustness depending on the perturbation procedure. Across 100 K-means fits using different random seeds, the three-cluster partition was reproduced exactly (ARI = 1.000 in all repetitions), indicating strong stability with respect to algorithm initialization. However, the observation-level sensitivity analysis produced a more heterogeneous pattern. Across 500 randomly selected 80% subsamples (n = 129), the median ARI was 1.000, whereas the empirical 2.5th–97.5th percentile range extended from approximately 0.200 to 1.000. Although the median indicated substantial agreement with the reference partition, the lower tail demonstrated that cluster membership could change considerably under some reductions in the analyzed observations. Accordingly, the solution was considered highly reproducible with respect to initialization but not uniformly stable under changes in sample composition.

The exploratory sample-relative portfolio-burden scores revealed considerable variation among the 161 administrative units under the baseline analytical specification. Odžaci (IPDRI = 100.00), Tutin (99.49), and Niš (98.96) exhibited the highest observed scores within this dataset. However, these values represent relative positions in the constructed portfolio-burden distribution and should not be interpreted as definitive rankings of disaster risk or expected disaster losses. Specifically, Odžaci and Niš were classified as Moderate under the supplied STAR assessment, whereas Tutin was classified as High; nevertheless, all three were positioned in the upper sample quartile of IPDRI, demonstrating that the exploratory portfolio-burden classification should not be confused with the official STAR risk category. The 20 local administrative units with the highest baseline IPDRI scores are presented in Table 21 for descriptive purposes and should not be interpreted as a definitive risk-prioritization list.

Table 21. Twenty local administrative units with the highest Integrated Portfolio Disaster Risk Index.

Rank	District	Local Unit	IPDRI	PRB	CHEB	PIP	STAR Risk	Burden Class	Cluster
1	Zapadno-Bački	Odžaci	100.00	49.19	5.47	9.00	3	Very high	1
2	Raški	Tutin	99.49	48.95	4.08	12.00	4	Very high	1
3	Nišavski	Niš	98.96	48.70	5.41	9.00	3	Very high	1
4	Nišavski	Aleksinac	87.69	43.39	4.82	9.00	3	Very high	1
5	Pčinjski	Trgovište	86.73	42.94	4.77	9.00	3	Very high	1
6	Mačvanski	Krupanj	86.12	42.65	4.74	9.00	3	Very high	1
7	Mačvanski	Mali Zvornik	86.12	42.65	4.74	9.00	3	Very high	1
8	Pčinjski	Bosilegrad	85.51	42.36	4.71	9.00	3	Very high	1
9	Pčinjski	Vranje	84.23	41.76	4.64	9.00	3	Very high	1
10	Mačvanski	Koceljeva	83.06	41.21	4.58	9.00	3	Very high	1
11	Mačvanski	Ljubovija	80.39	39.95	4.44	9.00	3	Very high	1
12	Zlatiborski	Sjenica	79.10	39.34	4.37	9.00	3	Very high	1
13	Jablanički	Crna Trava	79.09	39.34	4.37	9.00	3	Very high	1
14	Zlatiborski	Prijepolje	78.23	38.93	4.33	9.00	3	Very high	1
15	Mačvanski	Bogatić	76.41	38.08	4.23	9.00	3	Very high	1
16	Zapadno-Bački	Sombor	74.46	37.16	4.13	9.00	3	Very high	1
17	Nišavski	Doljevac	73.48	36.70	4.08	9.00	3	Very high	1
18	Pčinjski	Surdulica	71.58	35.80	3.98	9.00	3	Very high	1
19	Nišavski	Svrljig	71.50	35.77	3.97	9.00	3	Very high	1
20	Moravički	Ivanjica	71.30	35.67	3.96	9.00	3	Very high	1

Note. STAR risk represents the supplied official risk category, whereas the IPDRI burden class is an exploratory, sample-relative quartile classification. "Very high" denotes the upper sample quartile of portfolio burden, not an official WHO STAR risk category, a prediction of imminent danger, or a public-warning threshold.

5. Discussion

5.1. Principal Findings and Contribution

This nationwide secondary analysis yields four findings with direct methodological and policy significance. First, the Serbian STAR profile is nationally concentrated in the moderate risk category but is characterized by substantial district-level heterogeneity. Second, the observed associations among probability, frequency, impact, vulnerability, coping-capacity score, and risk are consistent with the STAR architecture but cannot be interpreted as independent causal effects because several variables are formative components of the same scoring system. Third, exposure-weighted portfolio burden—captured through CHEB, PRB, and the sample-relative IPDRI—behaves differently from the supplied STAR risk category. Fourth, multiplying aggregate probability by aggregate impact reproduces the supplied risk category only imperfectly, indicating potential aggregation-related differences that require further verification using hazard-level records. Importantly, PIP, CHEB, exposure-weighted PIP, PRB, IPDRI, structural susceptibility, hazard dynamics, and K-means profiles are author-derived analytical extensions rather than official WHO STAR indicators or independently validated risk measures.

These findings extend recent STAR research in two ways. Existing STAR applications emphasize hazard prioritization, participatory consensus, and the translation of risk profiles into preparedness action [37,38,40]. The present study adds a subnational statistical perspective by examining the spatial distribution and internal structure of the resulting local profiles. It also complements Yota et al. [39], who showed that STAR's correspondence with observed emergencies varies across hazards and contexts, by

demonstrating that analytical interpretation is additionally affected by geographic aggregation and by the distinction between risk intensity and cumulative exposure burden.

5.2. National Moderation Can Coexist with Pronounced Subnational Heterogeneity

The dominance of the moderate STAR category should not be interpreted as territorial homogeneity or as evidence that local preparedness needs are similar. District membership explained a large share of variation in the supplied risk level and even larger shares for several component and derived measures. Comparable place-based studies show that national averages routinely conceal substantial local variation in vulnerability, exposure, resilience, and capacity [51,52,55,56]. The same principle underlies the local administrative-unit emphasis in risk-informed planning frameworks [57,59].

The GIS results reinforce this interpretation by making municipality-level heterogeneity directly visible. Although the moderate STAR category dominates nationally, the spatial distribution of low and high categories is uneven, while population exposure exhibits substantially greater local differentiation. This spatial contrast illustrates why national or district-level summary statistics alone may not fully describe the territorial configuration of public-health emergency risk.

For Serbia, this pattern is consistent with earlier evidence of uneven preparedness and resilience across municipalities and regions. Local-government capacity research identified variability in strategic, financial, policy, partnership, and communication functions [41], while the recent BRIC–DROP analysis reported spatial differences in perceived resilience and persistent gaps in warning, financing, evacuation, and rapid decision-making [43]. Qualitative evidence also points to uneven institutional cooperation and strong dependence on central authorities [44]. The present STAR analysis provides an independent operational assessment that converges on the conclusion that public-health preparedness should be territorially differentiated.

The size of the district effects is also relevant for governance. Disaster-risk management is implemented through multilevel systems in which national standards must be translated into local action. Where local data systems, financing, professional capacity, partnerships, or institutional mandates differ, a standardized assessment tool may still produce strongly heterogeneous profiles [26–29]. The finding therefore supports the Sendai emphasis on disaggregated risk information and risk-informed local planning rather than a single national classification [30,33,36].

An important methodological consideration concerns the modifiable areal unit problem (MAUP), which may affect the interpretation of geographic differences in risk assessment results. MAUP includes both scale effects, whereby analytical outcomes vary according to the spatial level of aggregation, and zoning effects, whereby results change when geographic boundaries or administrative groupings are modified. In the present study, the 161 administrative units were heterogeneous in territorial extent, population characteristics, institutional responsibilities, and potentially in hazard-identification opportunities. This issue is particularly relevant to comparisons between the 17 municipalities of the City of Belgrade and other local self-government units. Differences in hazard counts, reported exposure proportions, and derived portfolio-burden scores may therefore reflect not only underlying risk characteristics but also the spatial and administrative structure of the assessment units. Although the use of exposure proportions and standardized indicators facilitates descriptive comparison, these procedures do not eliminate MAUP or establish equivalence between administrative units. Accordingly, the observed territorial contrasts should not be interpreted as evidence of intrinsic differences in underlying risk independently of spatial scale and administrative context.

5.3. Component Associations, Formative Dependence, and the Correct Interpretation of Coping Capacity

Probability showed the strongest association with the supplied risk category, followed by frequency, vulnerability, impact, and coping-capacity score. From a substantive perspective, these relationships are expected; from a statistical perspective, they require careful qualification. STAR is not a set of independent psychometric predictors. Probability and impact define the hazard-specific risk matrix, frequency contributes to probability assessment, and vulnerability and coping capacity contribute to impact. Strong coefficients for these components therefore partly reflect the instrument's construction. Similar caution is recommended more generally for composite risk and resilience indices, where part-whole correlations can be mistaken for independent explanatory mechanisms [50,51,53].

The relatively large odds ratio for probability in the cumulative-logit sensitivity model should not be interpreted as evidence that actual emergency occurrence increases fivefold. The estimate reflects a conditional association with the supplied ordinal STAR risk classification, within which probability is already a constituent assessment dimension. Moreover, only nine administrative units occupied the highest observed risk category, limiting the information available for upper-category contrasts. Consequently, the magnitude of this association was considered sensitive to model assumptions and the formative structure of STAR rather than evidence of an independent substantive effect.

The reanalysis also resolves an important substantive error in the source interpretation. Under the official Serbian STAR methodological guidance, coping capacity is inverse-coded: 1 denotes very high capacity and 5 very low capacity. A positive association between the numerical coping-capacity score and risk therefore means that poorer capacity accompanies higher risk, not that stronger capacity increases risk. This direction is consistent with resilience theory, which treats available resources, organizational linkages, social capital, information, and adaptive capability as protective assets [61–64].

Nevertheless, coping capacity should not be overinterpreted as an independent coefficient in the adjusted models. Its range is restricted, it is already embedded in the impact pathway, and the available dataset contains no usable variation in the separate managerial, health-sector, non-health-sector, and community subcapacity fields. The health-system literature indicates that these subdomains may have different operational roles—governance, financing, workforce, information, service delivery, partnerships, and community functions do not necessarily move together [7,9–11]. These limitations have important implications for local disaster-risk governance. The remaining ordinal coping-capacity score cannot independently characterize staffing and leadership, interagency coordination, institutional trust, social cohesion, volunteer networks, or psychosocial resources. Consequently, local authorities should interpret STAR-derived risk scores as inputs to preparedness planning rather than comprehensive measures of organizational and societal coping capacity. Technical risk assessments should be complemented by documented capacity audits, assessments of available personnel and response resources, community consultations, interagency exercises, and qualitative evaluations of institutional and community preparedness. Future Serbian STAR assessment cycles should preserve disaggregated capacity scores, clear variable definitions, missing-value codes, and source documentation so that unavailable information can be distinguished from genuinely weak capacity.

5.4. Risk Intensity and Exposure-Weighted Portfolio Burden Are Complementary Dimensions

The most important analytical extension is separating probability-impact intensity from cumulative portfolio/exposure burden. The supplied STAR category is

fundamentally organized around probability and impact. By contrast, CHEB and IPDRI incorporate the number of identified hazards and the reported unit-level exposure proportion. The weak IPDRI–STAR association indicates limited correspondence between the two assessment representations in the present dataset, without demonstrating that they measure independent underlying risk dimensions. A jurisdiction can carry a broad multi-hazard burden with substantial population exposure while remaining in a moderate aggregate probability-impact category.

The GIS-based results provided a descriptive geographic representation of variation in CHEB, IPDRI, and exploratory local risk profiles across Serbian administrative units. The thematic maps revealed geographically uneven distributions of the constructed portfolio-burden measures, while the exploratory cluster map illustrated the locations of administrative units assigned to different attribute-based profiles. However, these visual patterns should not be interpreted as evidence of statistically significant spatial clustering, spatial autocorrelation, or geographic hotspots. K-means clustering identified similarities in assessment characteristics rather than spatial proximity. Therefore, the geographic visualizations complement the statistical analysis by illustrating the territorial distribution of observed attributes without establishing spatial dependence.

This distinction is consistent with multi-hazard theory. Drakes and Tate [16] show that aggregate, compound, and cascading multi-hazard perspectives emphasize different dimensions of vulnerability. Pescaroli and Alexander [17], Gill and Malamud [18], and van den Hurk et al. [20] similarly caution that treating hazards independently can overlook risk interactions and cumulative consequences. Global evidence that multi-hazard events drive disproportionate losses and affect populations reinforces the need to consider portfolio and interaction effects [21,22].

The derived IPDRI should be interpreted exclusively as an exploratory, sample-relative measure of constructed portfolio burden rather than a general disaster risk index, an official WHO STAR indicator, or a calibrated estimate of expected loss. Its values and resulting administrative-unit ordering depend on the observed PRB distribution and the selected indicator construction and normalization procedures. Consequently, the identification of units with comparatively high IPDRI scores does not establish that these units face the highest absolute disaster risk or should automatically receive the highest preparedness priority. Nevertheless, the measure provides a descriptive representation of how hazard-portfolio breadth and population exposure contribute to variation within the analyzed assessment dataset. Such information may complement the supplied STAR risk classification, provided that it is interpreted alongside vulnerability, coping capacity, data confidence, local context, and the limitations of composite-indicator construction [6,65–67,77]. It lacks hazard-specific population overlap, mortality, morbidity, duration, economic loss, temporal dependence, and interaction terms. Its value is more limited and more defensible: it provides an alternative descriptive ordering of administrative units based on hazard count and reported exposure, without demonstrating incremental predictive validity or an independently established risk dimension. This use is consistent with the composite-index literature, in which alternative indices can illuminate different policy dimensions if their construction and limitations are explicit [6,65–67,77].

The absence of a separate capacity divisor in PRB should not be interpreted as implying that coping capacity or community resilience has no protective role. Rather, capacity is indirectly incorporated through the supplied STAR impact score, and the present analytical construction does not allow its independent buffering effect to be estimated. Moreover, the available managerial, health-sector, non-health-sector, and community subcapacity fields contained no informative variation and could not support a disaggregated assessment of capacity. Future research should therefore incorporate independently measured, appropriately scaled indicators of health-system preparedness,

institutional response capabilities, and community resilience, alongside observed emergency outcomes, before developing and validating explicitly capacity-adjusted risk models.

The strong association between CHEB and IPDRI is mathematically expected because CHEB is part of the PRB/IPDRI construction; it is evidence of construct composition, not independent validation. The weak observed association between IPDRI and the supplied STAR risk category provides a descriptive indication of limited correspondence between these two representations within the analyzed dataset. Similarly, differences in STAR risk, PIP, and impact across the exploratory clusters should be interpreted as internal profile characteristics rather than evidence of external validity. Although the supplied STAR risk category was not used directly as a clustering input, its constituent assessment pathways overlap with several clustering variables. Consequently, neither the observed cluster differences nor the correlations among the constructed indicators demonstrate predictive accuracy, independent construct validity, or the existence of externally validated risk typologies. This mirrors evidence that vulnerability and resilience indices may show limited empirical overlap even when both are important for planning [60]. Accordingly, the observed relationships should be understood at three distinct analytical levels. First, the relationships among derived measures reflect their algebraic construction and therefore do not provide independent evidence of validity. Second, associations between the constructed measures and the supplied STAR categories describe patterns within the same assessment dataset, without demonstrating predictive performance or independent construct validity. Third, genuine external validation would require comparison with independently documented public health emergencies, observed disaster impacts, or operational response outcomes. Because such independent outcome data were unavailable, the present findings support a descriptive comparison of alternative risk representations rather than the empirical validation of a new risk assessment instrument.

5.5. PIP–STAR Discordance and Aggregation Uncertainty

Applying the official STAR risk-matrix thresholds to aggregate probability × aggregate impact reproduced the supplied risk category in 75.8% of local units, with moderate weighted agreement. This discrepancy does not establish an error in STAR implementation or identify its precise cause. Differences in aggregation procedures, rounding, or other source-data processing decisions may contribute to the observed disagreement, but these possibilities cannot be independently verified without hazard-level records.

This finding has broader implications for reproducibility. Composite-indicator research repeatedly demonstrates that aggregation rules can change rankings and interpretation [50–52]. STAR publications should therefore specify whether municipality-level component values are means, maxima, medians, weighted summaries, or other aggregations; preserve hazard-level records wherever possible; and clearly distinguish hazard-specific risk, portfolio summary risk, and any analytically reconstructed score. Multi-hazard risk modeling and data-scarce national assessments increasingly emphasize similar transparency [25,71].

The non-circular regression analyses reinforce this interpretation. When constitutive probability, impact, vulnerability, and coping capacity were deliberately excluded, exposure burden and macroregion explained little of aggregate PIP. At the same time, the exploratory ordered model suggested that exposure burden and the supplied categorical risk can move in different directions. The two measures should therefore be treated as distinct outputs serving different planning questions rather than competing estimates of the same latent quantity.

5.6. Implications for Public-Health Preparedness, Local Governance, and Risk Communication

The results support a preparedness model in which risk assessment is linked directly to differentiated action. Local units with high probability-impact intensity may require hazard-specific prevention, surveillance, clinical readiness, and rapid-response planning; units with high portfolio/exposure burden may additionally require broader surge capacity, cross-sector logistics, continuity planning, and prioritization of vulnerable populations. This approach aligns with resilience-based preparedness frameworks that emphasize governance, partnerships, information systems, workforce, equity, and the ability to adapt under pressure [7,8,15,84].

Regional coordination is equally important. Strong local variation supports shared capacities, regional professional networks, mutual aid, harmonized surveillance, and cross-jurisdictional learning. Evidence from public-health regionalization and emergency-management collaboration suggests that such arrangements can improve planning and resource efficiency when roles, authority, trust, and communication are clear [9,26,27]. At the governance level, fragmented or top-down arrangements can weaken participation and adaptive capacity, particularly in complex or cascading crises [24,31,32,69].

Data confidence deserves similar policy attention. It displayed one of the strongest territorial patterns in the Serbian dataset. Variation in confidence may reflect differences in surveillance, documentation, access to local evidence, institutional information exchange, or the maturity of assessment teams. Dynamic preparedness approaches emphasize revisiting risk profiles as data and conditions change [13]. Yota et al. [39] likewise argue for integration of real-time surveillance, climate information, seasonality, and finer geographic resolution to strengthen STAR use.

Risk communication and community engagement should be treated as core preparedness capacities rather than peripheral dissemination functions. Systematic reviews consistently support locally grounded engagement, two-way communication, trusted messengers, community feedback, and inclusion [96–98,100]. Early-warning research shows that technology without sustained community engagement leaves important gaps in response capability [99]. Health-emergency evidence similarly stresses that communities should be involved before crises, not only informed during them [101–104].

Trust provides a cross-cutting mechanism. Bonfanti et al. [108] identify trust as central across prevention, preparedness, response, and recovery, while Nicholas et al. [109] demonstrate that its effects vary by context and by the institution or actor in whom trust is placed. For Serbia, findings near the Duboko landfill show that transparency and access to information are linked to perceived trust and resilience [45]. Standardized risk assessment should therefore be accompanied by transparent communication about evidence quality, uncertainty, scoring logic, and the reasons behind preparedness priorities. To prevent misinterpretation of discrepant risk indicators, multilevel risk governance should distinguish clearly between the supplied official WHO STAR risk category and the exploratory, sample-relative IPDRI score. For example, Odžaci and Niš were classified as Moderate under STAR, whereas Tutin was classified as High, although all three belonged to the upper sample quartile of portfolio burden. Such quartile classifications should be communicated as relative portfolio-burden positions rather than as independent warnings of very high disaster risk. User-centered dashboards and institutional briefings should present both indicators in separately labeled fields, accompanied by the assessment date, calculation method, normalization reference population, data-confidence information, capacity-coding direction, and relevant methodological limitations. Apparent discrepancies should be reviewed collaboratively with local assessment teams, public-health institutions, emergency services, and community representatives to support transparency, institutional trust, and informed

interpretation. A high IPDRI position should prompt further examination of hazard-specific exposure, available response capacity, and data quality, rather than automatically triggering public alerts, resource-allocation decisions, or claims of imminent danger.

These policy implications are supported by both international theoretical perspectives and empirical disaster-risk research. Social-vulnerability scholarship, disaster sociology, and risk-perception research highlight the importance of societal conditions, institutional arrangements, and public understanding in interpreting technical risk assessments [110–112]. Cultural Theory of Risk and post-normal science further emphasize the relevance of differing social perspectives, uncertainty, and stakeholder participation in risk-governance processes [113,114]. Applied research demonstrates the importance of local governance capacity and community perspectives [115,116], while disaster-communication studies highlight the operational value of accessible warning systems, timely information, and sustained community engagement [117,119–121]. More broadly, international research on emergency coordination, place-based resilience measurement, disability-inclusive disaster risk reduction, and critical-infrastructure interdependencies reinforces the need for integrated and context-sensitive preparedness planning [93,123–125].

5.7. Relevance for Serbia and Southeast Europe

The Serbian results should be interpreted within a broader regional transition from emergency response toward risk-informed prevention and resilience. Previous Serbian research has repeatedly identified the need to strengthen local capacities, planning, public participation, and communication [41,42,46,47]. The recent BRIC–DROP and qualitative resilience studies further show that community resilience cannot be reduced to a single institutional or social indicator and that weaknesses in warning, financing, evacuation readiness, and local coordination remain salient [43,44].

These findings are not unique to Serbia. Comparative evidence from Bulgaria, Romania, and Albania identifies similar tensions between formal frameworks and operational local capacity [49]. Romanian spatial risk research also demonstrates pronounced local variation when multi-hazard exposure is combined with social vulnerability [56]. This regional context increases the transferability of the present study: a standardized all-hazards tool can provide a common assessment language, but scientific and policy interpretation still requires attention to local exposure, capacity, evidence quality, and aggregation.

Three policy implications follow. First, Serbia should maintain repeated STAR cycles and link them to interoperable local and national surveillance rather than treat the 2024 profiles as static classifications. Second, preserve hazard-level data and subdomain capacity scores in an analysis-ready format so changes in risk and preparedness can be evaluated longitudinally. Third, resource prioritization should use a dashboard of complementary indicators—risk intensity, exposure-weighted portfolio burden, vulnerability, coping capacity, and data confidence—rather than a single ranking. Such an approach is more consistent with contemporary systemic-risk and resilience governance [23,29,94].

5.8. Limitations and Research Agenda

Several limitations constrain interpretation. The design is cross-sectional and ecological; associations among local-level scores cannot establish causal effects or individual-level relationships. STAR relies on structured expert assessment and available evidence, so comparability depends on local information quality, facilitation, and consensus processes. Several variables have restricted ranges, reducing discrimination and statistical power. The available spreadsheet contains municipality-level summaries

rather than hazard-level records, preventing exact reconstruction of the original hazard-specific scoring and limiting analysis of within-unit hazard diversity. The cumulative-logit sensitivity models were additionally constrained by the small number of observations in the highest observed STAR risk category (n = 9) and the assumed proportional-odds structure. Accordingly, the estimated odds ratios should not be generalized to actual emergency occurrence or interpreted as independent causal effects.

A further limitation arises from administrative-scale heterogeneity and the modifiable areal unit problem (MAUP). The dataset combined 144 local self-government units with 17 municipalities within the City of Belgrade, which may differ in territorial extent, population size, institutional mandates, and assessment practices. Consequently, observed geographic contrasts and derived index rankings may be sensitive to the spatial units used for analysis. In particular, comparisons between Belgrade municipalities and other administrative units may be confounded by differences in administrative scale and institutional context. Neither the use of exposure proportions nor statistical standardization eliminates these limitations. Because harmonized hazard-level, population, and alternative spatial-aggregation data were unavailable for this analysis, we could not determine the extent to which the observed differences reflected genuine risk variation rather than administrative-scale effects. Future research should examine the sensitivity of assessment results to alternative spatial aggregations and harmonized territorial units.

An additional limitation concerns the absence of formal spatial-dependence testing. Although GIS-based thematic maps illustrated geographic variation in the assessed indicators, no global or local spatial autocorrelation statistics, hotspot detection procedures, or spatial scan analyses were performed. Consequently, the study cannot establish whether neighboring administrative units exhibit statistically significant similarities or differences beyond those expected by chance. Moreover, potential unmodeled spatial dependence could affect the uncertainty estimates and statistical inference obtained from conventional group comparisons and regression models. Future research should incorporate spatial weights, formal autocorrelation diagnostics, and appropriate spatial statistical models to evaluate these relationships.

The derived PIP, CHEB, PRB, and IPDRI measures are exploratory. They are not WHO-validated metrics, actuarial risk estimates, expected-loss functions, or substitutes for hazard-specific STAR assessment. The aggregation procedure underlying the reported exposure proportion could not be independently verified, and information on overlapping hazard-specific exposure footprints was unavailable. Consequently, CHEB represents a nominal hazard–exposure portfolio descriptor rather than a de-duplicated population percentage or count of uniquely exposed residents. It does not measure hazard simultaneity, observed event frequency, or temporal accumulation. Emergency managers should therefore use CHEB for exploratory comparisons of local hazard portfolios, not for estimating the number of people requiring assistance. Such estimates would require population denominators and hazard-specific spatial exposure data that allow overlapping populations to be identified. IPDRI is a sample-relative rescaling whose values should not be compared directly across countries or assessment cycles without recalibration. An additional limitation concerns the sample-relative construction and interpretation of IPDRI. Because the index was normalized using the observed minimum and maximum PRB values among the 161 administrative units, its scores and resulting rankings are dependent on the baseline dataset and analytical specification. The endpoints of the scale do not represent absolute risk thresholds, and quartile-based burden categories should not be interpreted as externally calibrated risk levels. Changes in the included administrative units, indicator definitions, aggregation rules, or normalization procedures may alter relative scores, class membership, and rankings. Accordingly, the

list of the twenty highest-scoring units should be regarded as an exploratory descriptive output rather than a definitive risk ranking or an independently validated basis for resource allocation. K-means typologies also treat standardized ordinal inputs as approximately interval and are therefore descriptive. Although the exploratory three-cluster solution showed strong internal reproducibility and agreement with Ward's hierarchical clustering under the examined specifications, these findings should not be interpreted as evidence of externally validated risk types. The pronounced imbalance in cluster sizes (137, 14, and 10 units), restricted variation in several ordinal STAR indicators, and reliance on standardized assessment scores limit the substantive interpretation of the resulting profiles. Moreover, algorithmic agreement does not establish cluster stability under changes in the underlying observations, the existence of natural population subgroups, or the operational usefulness of the classification. The exploratory clustering results should also be interpreted in light of their differing stability properties. Although repeated K-means initializations consistently reproduced the reference partition, subsampling revealed substantial variability in some solutions. This distinction indicates that algorithmic reproducibility does not necessarily imply robustness to changes in the observed administrative units. The pronounced cluster-size imbalance limits operational discrimination because 85.1% of administrative units belong to a single group. This asymmetry may partly reflect the restricted variation in ordinal vulnerability and coping-capacity scores, where rare categories can exert disproportionate influence on Euclidean distances after standardization. However, this mechanism cannot be established conclusively from the present clustering results. The agreement between K-means and Ward clustering, both applied to the same standardized inputs, demonstrates internal algorithmic consistency rather than independent validation. Future research should compare ordinal-aware dissimilarities, mixed-data clustering approaches, and more detailed hazard-level profiles to determine whether alternative specifications provide greater stability and operational discrimination. Until such comparisons and external validation are available, the three clusters should be interpreted as exploratory descriptive profiles rather than definitive or generalizable risk typologies.

Future research should retain the hazard as the primary analytical unit and use longitudinal assessment cycles to evaluate temporal change. Validation against observed outbreaks, emergency activations, morbidity, mortality, service disruption, or disaster losses would allow stronger assessment of predictive or criterion validity. Dynamic or Bayesian multi-hazard approaches could incorporate interactions, changing vulnerability, and infrastructure dependencies [19,68,70]. A mixed-method design could additionally explain why units with similar categorical risk have different capacity or portfolio-burden profiles, thereby combining the strengths of quantitative standardization with context-sensitive local knowledge [44,95].

Finally, future STAR research should evaluate the consequences of aggregation itself. Comparing hazard-level, municipality-level, district-level, and national summaries would clarify when information is lost or rankings change. Sensitivity analysis of alternative aggregation rules, uncertainty propagation, and repeated assessment under updated data would bring STAR-based research into closer alignment with current best practice in composite-indicator and multi-hazard science [23,50,51,76].

6. Conclusions

This cross-sectional ecological analysis of the supplied 2024 WHO STAR assessment summaries for 161 Serbian local administrative units identified a predominantly moderate public-health emergency risk classification alongside substantial territorial heterogeneity. Local units and districts differed in their assessed probability, frequency, impact, vulnerability, coping capacity, and reported exposure. Thus, similar supplied risk

categories may coexist with differing combinations of assessment characteristics. GIS-based thematic maps provided a descriptive representation of these territorial differences, but the study did not test spatial autocorrelation or establish statistically significant geographic clustering.

Probability and frequency showed the strongest observed associations with the supplied risk categories, while vulnerability, impact, and coping-capacity scores contributed to variation in the assessed profiles. These relationships should not be interpreted as independent causal effects because several components contribute directly or indirectly to the STAR scoring process. Moreover, applying a probability–impact cross-product to the available local-unit summary scores did not fully reproduce the supplied STAR categories. This discrepancy indicates that such a reconstructed score is not interchangeable with the reported classification; without hazard-level records and documented aggregation rules, its precise source cannot be established.

A further contribution of the study is the descriptive comparison of categorical risk assessments with author-derived exposure-weighted portfolio measures. CHEB, PRB, and the sample-relative IPDRI displayed territorial variation and limited correspondence with the supplied STAR risk category, indicating that units assigned similar categories can receive different constructed burden scores. However, these differences do not establish independent underlying risk dimensions or quantify the number of unique residents exposed. The derived measures depend on the selected formulas, reported exposure summaries, aggregation assumptions, and composition of the study sample. Specifically, IPDRI is min–max normalized using the observed PRB range within the 161-unit Serbian dataset assessed in 2024. Its values do not represent absolute risk levels, event probabilities, or expected losses and cannot be compared directly across countries or assessment cycles without recalibration and harmonization of the underlying indicators and assessment procedures. Accordingly, the derived measures should be considered exploratory supplements to, rather than validated replacements for, official STAR outputs.

Exploratory clustering provided another way to summarize combinations of the observed assessment characteristics beyond a single ordered risk classification. The resulting profiles may help identify questions for further local investigation, including whether comparatively elevated exposure, vulnerability, hazard frequency, or weaker coping capacity coincide in particular units. Nevertheless, the clusters are dependent on the selected variables and analytical specification, are not statistically verified spatial clusters, and have not been externally validated as planning categories. Administrative-scale differences, including those between Belgrade municipalities and other local government units, further limit direct comparisons.

Taken together, the findings suggest that public-health emergency preparedness discussions in Serbia could benefit from reviewing supplied STAR categories alongside disaggregated component scores, reported exposure, and cautiously interpreted portfolio summaries. Such a multidimensional description may help frame questions about prevention, surveillance, surge capacity, risk communication, and intermunicipal coordination, but it does not demonstrate superior predictive accuracy or provide an optimal rule for prioritizing investments or allocating resources. Stronger operational conclusions will require access to documented hazard-level assessments, more complete capacity data, verification of exposure aggregation, sensitivity analyses across administrative scales and index specifications, repeated assessment cycles, and validation against independent emergency, health, and service-disruption outcomes.

Supplementary Materials: The following supporting information can be downloaded at: https://www.mdpi.com/article/10.3390/safety12060145/s1, Supplementary Tables S1–S6 (additional

statistical results and municipality-level data); Supplementary Figures S1–S10 (GIS-based thematic maps).

Author Contributions: Conceptualization, V.M.C. and D.I.; methodology, V.M.C., D.I. and T.L.; validation, V.M.C., D.I., V.L., J.B. and V.D.C.; formal analysis, V.M.C. and V.D.C.; investigation, D.I. and J.B.; resources, D.I.; data curation, D.I. and V.M.C.; writing—original draft preparation, V.M.C.; writing—review and editing, V.M.C., D.I., V.L., L.S., J.B., T.L. and V.D.C.; visualization, V.M.C., L.S. and V.D.C.; supervision, V.M.C.; project administration, V.M.C. and D.I. All authors have read and agreed to the published version of the manuscript.

Funding: T.L. acknowledges support from the Program of Cooperation with the Serbian Scientific Diaspora—Joint Research Projects—DIASPORA 2023, from the Science Fund of the Republic of Serbia, under the project LAMINATION (The Loess Plateau Margins: Towards Innovative Sustainable Conservation), Project number: 17807. Also, this research was supported by the Scientific-Professional Society for Disaster Risk Management, Belgrade, Serbia (https://spsdrm.org/, accessed on 1 September 2026); the International Institute for Disaster Research, Belgrade, Serbia (https://idr.edu.rs/, accessed on 1 September 2026); and ProSafeNet—The Global Hub for Safety, Security, Risk & Emergency Professionals & Scientists (https://prosafenet.com/, accessed on 1 September 2026).

Institutional Review Board Statement: Not applicable.

Informed Consent Statement: Not applicable.

Data Availability Statement: All aggregate data and statistical results supporting the findings of this study are reported in the article and the Supplementary Materials.

Acknowledgments: The authors acknowledge the use of Grammarly Premium v1.2.291.1949 and ChatGPT 5.6 for language editing and improving the clarity of the English text. Canva AI was used to assist with the visual design of schematic Figures 1–3. The scientific concepts, methodological relationships, and final content of these figures were reviewed and verified by the authors. The authors take full responsibility for the accuracy, originality, and integrity of the manuscript.

Conflicts of Interest: The authors declare no conflicts of interest.

References

1. Adger, W.N. Vulnerability. *Glob. Environ. Change* **2006**, *16*, 268–281. https://doi.org/10.1016/j.gloenvcha.2006.02.006.
2. Cutter, S.L.; Boruff, B.J.; Shirley, W.L. Social vulnerability to environmental hazards. *Soc. Sci. Q.* **2003**, *84*, 242–261. https://doi.org/10.1111/1540-6237.8402002.
3. Flanagan, B.E.; Gregory, E.W.; Hallisey, E.J.; Heitgerd, J.L.; Lewis, B. A social vulnerability index for disaster management. *J. Homel. Secur. Emerg. Manag.* **2011**, *8*, 3. https://doi.org/10.2202/1547-7355.1792.
4. Keim, M. Building human resilience: The role of public health preparedness and response as an adaptation to climate change. *Am. J. Prev. Med.* **2008**, *35*, 508–516. https://doi.org/10.1016/j.amepre.2008.08.022.
5. Keim, M. Defining disaster-related health risk: A primer for prevention. *Prehospital Disaster Med.* **2018**, *33*, 308–316. https://doi.org/10.1017/S1049023X18000390.
6. Marin, G.; Modica, M.; Paleari, S.; Zoboli, R. Assessing disaster risk by integrating natural and socio-economic dimensions: A decision-support tool. *Socio-Econ. Plan. Sci.* **2021**, *77*, 101032. https://doi.org/10.1016/j.seps.2021.101032.
7. Khan, Y.; O'sullivan, T.; Brown, A.; Tracey, S.; Gibson, J.; Généreux, M.; Henry, B.; Schwartz, B. Public health emergency preparedness: A framework to promote resilience. *BMC Public Health* **2018**, *18*, 1344. https://doi.org/10.1186/s12889-018-6250-7.
8. Khatri, R.; Endalamaw, A.; Erku, D.; Wolka, E.; Nigatu, F.; Zewdie, A.; Assefa, Y. Preparedness, impacts, and responses of public health emergencies towards health security: Qualitative synthesis of evidence. *Arch. Public Health* **2023**, *81*, 208. https://doi.org/10.1186/s13690-023-01223-y.
9. Gooding, K.; Bertone, M.; Loffreda, G.; Witter, S. How can we strengthen partnership and coordination for health system emergency preparedness and response? Findings from a synthesis of experience across countries facing shocks. *BMC Health Serv. Res.* **2022**, *22*, 1441. https://doi.org/10.1186/s12913-022-08859-6.

10. Sasie, S.D.; Aragaw, F.M.; Gebeyehu, T.A.; Shikur, S.A.; Fekadu, L.; Ali, N.Z.; Argaw, Z.M. Building systems for preparedness: Global scoping studies on institutional governance and National Public Health Agencies. *PLoS Glob. Public Health* **2026**, *6*, e0005427. https://doi.org/10.1371/journal.pgph.0005427.
11. El-Jardali, F.; Kanth, P.D.; Nguyen, S.-N.; Varkey, S.; Duran, D.; Menon, R.; Fadlallah, R.; Malek, A.; Jain, V.; Saleh, M.; et al. Emergency preparedness and health system resilience assessment tool: Development and initial validation. *BMJ Glob. Health* **2025**, *10*, e016459. https://doi.org/10.1136/bmjgh-2024-016459.
12. Kruk, M.E.; Myers, M.; Varpilah, S.T.; Dahn, B.T. What is a resilient health system? Lessons from Ebola. *Lancet* **2015**, *385*, 1910–1912. https://doi.org/10.1016/S0140-6736(15)60755-3.
13. Kandel, N.; Chungong, S. Dynamic preparedness metric: A paradigm shift to measure and act on preparedness. *Lancet Glob. Health* **2022**, *10*, e615–e616. https://doi.org/10.1016/S2214-109X(22)00097-3.
14. Plough, A.; Fielding, J.E.; Chandra, A.; Williams, M.; Eisenman, D.; Wells, K.B.; Law, G.Y.; Fogleman, S.; Magaña, A. Building community disaster resilience: Perspectives from a large urban county department of public health. *Am. J. Public Health* **2013**, *103*, 1190–1197. https://doi.org/10.2105/AJPH.2013.301268.
15. Peterson, L.N.; Baggett, J.; Evans, A.; Sullivan, K. Evidence-based strategies to enhance public health emergency preparedness and response. *J. Public Health Manag. Pract.* **2024**, *30*, 311–313. https://doi.org/10.1097/PHH.0000000000001879.
16. Drakes, O.; Tate, E. Social vulnerability in a multi-hazard context: A systematic review. *Environ. Res. Lett.* **2022**, *17*, 033001. https://doi.org/10.1088/1748-9326/ac5140.
17. Pescaroli, G.; Alexander, D. Understanding compound, interconnected, interacting, and cascading risks: A holistic framework. *Risk Anal.* **2018**, *38*, 2245–2257. https://doi.org/10.1111/risa.13128.
18. Gill, J.; Malamud, B. Hazard interactions and interaction networks (cascades) within multi-hazard methodologies. *Earth Syst. Dyn.* **2016**, *7*, 659–679. https://doi.org/10.5194/esd-7-659-2016.
19. de Ruiter, M.D.; van Loon, A.V. The challenges of dynamic vulnerability and how to assess it. *iScience* **2022**, *25*, 104720. https://doi.org/10.1016/j.isci.2022.104720.
20. van den Hurk, B.; White, C.; Ramos, A.; Ward, P.; Martius, O.; Olbert, I.; Roscoe, K.; Goulart, H.M.; Zscheischler, J. Consideration of compound drivers and impacts in the disaster risk reduction cycle. *iScience* **2023**, *26*, 106030. https://doi.org/10.1016/j.isci.2023.106030.
21. Lee, R.; White, C.J.; Adnan, M.S.G.; Douglas, J.; Mahecha, M.D.; O'LOughlin, F.E.; Patelli, E.; Ramos, A.M.; Roberts, M.J.; Martius, O.; et al. Reclassifying historical disasters: From single to multi-hazards. *Sci. Total Environ.* **2024**, *912*, 169120. https://doi.org/10.1016/j.scitotenv.2023.169120.
22. Jäger, W.S.; de Ruiter, M.D.; Tiggeloven, T.; Ward, P.J. What can we learn about multi-hazard impacts from global disaster records? *Nat. Hazards Earth Syst. Sci.* **2025**, *25*, 2751–2769. https://doi.org/10.5194/nhess-25-2751-2025.
23. Tiggeloven, T.; Raymond, C.; de Ruiter, M.C.; Sillmann, J.; Thieken, A.H.; Buijs, S.L.; Ciurean, R.; Cordier, E.; Crummy, J.M.; Cumiskey, L.; et al. Multi-hazard risk assessment and management: Pathways for the Sendai Framework and beyond. *Geosci. Commun.* **2026**, *9*, 185–221. https://doi.org/10.5194/gc-9-185-2026.
24. Liu, H.; Renn, O. Polycrisis and systemic risk: Assessment, governance, and communication. *Int. J. Disaster Risk Sci.* **2025**, *16*, 526–549. https://doi.org/10.1007/s13753-025-00636-3.
25. Leone, M.F.; Zuccaro, G.; De Gregorio, D.; Turchi, A.; Tedeschi, A.; Büegelmayer-Blaschek, M.; Sfetsos, A.; Zarikos, I.; Coronas, A.d.l.C.; Russo, B. A holistic asset-level modelling framework for a comprehensive multi-hazard risk/impact assessment: Insights from the ICARIA project. *Int. J. Disaster Risk Reduct.* **2025**, *119*, 105319. https://doi.org/10.1016/j.ijdrr.2025.105319.
26. Stoto, M.A. Regionalization in local public health systems: Variation in rationale, implementation, and impact on public health preparedness. *Public Health Rep.* **2008**, *123*, 441–449. https://doi.org/10.1177/003335490812300405.
27. Wolf-Fordham, S. Integrating government silos: Local emergency management and public health department collaboration for emergency planning and response. *Am. Rev. Public Adm.* **2020**, *50*, 560–567. https://doi.org/10.1177/0275074020943706.
28. Lee, D. Local government's disaster management capacity and disaster resilience. *Local Gov. Stud.* **2019**, *45*, 803–826. https://doi.org/10.1080/03003930.2019.1653284.
29. Dai, J.; Azhar, A. Collaborative governance in disaster management and sustainable development. *Public Adm. Dev.* **2024**, *44*, 358–380. https://doi.org/10.1002/pad.2071.
30. Djalante, R.; Lassa, S. Governing complexities and its implication on the Sendai Framework for Disaster Risk Reduction Priority 2 on governance. *Prog. Disaster Sci.* **2019**, *2*, 100010. https://doi.org/10.1016/j.pdisas.2019.100010.
31. Okunola, O.H. Beyond institutional silos: Rethinking multilevel disaster risk governance in Africa a decade into the Sendai Framework implementation. *Int. J. Disaster Risk Sci.* **2025**, *16*, 321–332. https://doi.org/10.1007/s13753-025-00646-1.

32. Okunola, O.H. Exploring multi-level governance arrangements in disaster recovery: A study of Lagos, Nigeria. *Int. J. Disaster Risk Reduct.* **2025**, *118*, 105254. https://doi.org/10.1016/j.ijdrr.2025.105254.
33. Mizutori, M. Reflections on the Sendai Framework for Disaster Risk Reduction: Five years since its adoption. *Int. J. Disaster Risk Sci.* **2020**, *11*, 147–151. https://doi.org/10.1007/s13753-020-00261-2.
34. Surianto, S.; Alim, S.; Nindrea, R.; Trisnantoro, L. Regional policy for disaster risk management in developing countries within the Sendai Framework: A systematic review. *Open Access Maced. J. Med. Sci.* **2019**, *7*, 2213–2219. https://doi.org/10.3889/oamjms.2019.614.
35. Nekoei-Moghadam, M.; Moradi, S.M.; Tavan, A. How can the Sendai Framework be implemented for disaster risk reduction and sustainable development? A qualitative study in Iran. *Glob. Health* **2024**, *20*, 23. https://doi.org/10.1186/s12992-024-01028-w.
36. Cabral-Ramírez, M.; Niño-Barrero, Y.; DiBella, J. Lessons from the implementation of the Sendai Framework for Disaster Risk Reduction from Latin America and the Caribbean. *Int. J. Disaster Risk Sci.* **2025**, *16*, 72–83. https://doi.org/10.1007/s13753-025-00613-w.
37. Awoyale, O.D.; Jimoh, A.; Dede, A.; Akpen, C.N.; Ogunniyi, A.; Dogo, D.P.; Gimba, P.B.; Ibrahim, I.; Rauf, R.; Mustafa, A.; et al. Strengthening disaster preparedness and health security in Niger State, Nigeria through a WHO STAR-based multi-hazard risk assessment. *Sci. Rep.* **2026**, *16*, 4607. https://doi.org/10.1038/s41598-025-34702-z.
38. Elhakim, M.; Hammoud, S.D.; Gmach, S.; Albadri, J.; Mahrous, H.; Arifi, F.; Latif, N.A.; Moussa, S.; Anan, H.; Saidouni, A.; et al. Learning interventions in the WHO Eastern Mediterranean region: Supporting Member States to get prepared for better response to health emergencies in the region. *Front. Public Health* **2024**, *12*, 1441223. https://doi.org/10.3389/fpubh.2024.1441223.
39. Yota, D.; Massidi, C.; Talisuna, A.; Tchikamgoua, O.N. Assessing the correlation between STAR health risk forecasts with actual health emergencies in West and Central Africa: A three-year analysis. *Front. Public Health* **2026**, *13*, 1728832. https://doi.org/10.3389/fpubh.2025.1728832.
40. Tomašević, T.; Ivanović, D.; Jovanović, V.; Ivanović, I.; Rančić, M.; Boban, J.; Perić, M.; Todorović, M. Public health risk assessments at the local government level in the Republic of Serbia. In Proceedings of the International Congress Public Health—Achievements and Challenges, Belgrade, Serbia, 15–16 October 2024. https://doi.org/10.5937/BatutPHCO24111T.
41. Cvetković, V.; Tanasić, J.; Ocal, A.; Kešetović, Ž.; Nikolić, N.; Dragašević, A. Capacity development of local self-governments for disaster risk management. *Int. J. Environ. Res. Public Health* **2021**, *18*, 10406. https://doi.org/10.3390/ijerph181910406.
42. Cvetković, V.M. A predictive model of community disaster resilience based on social identity influences (MODERSI). *Int. J. Disaster Risk Manag.* **2023**, *5*, 57–80. https://doi.org/10.18485/ijdrm.2023.5.2.5.
43. Cvetković, V.M.; Milenković, D.; Bašić, J.; Lukić, T.; Renner, R. Predictive model of community disaster resilience across Serbia: A BRIC–DROP composite index and spatial patterns. *Safety* **2026**, *12*, 59. https://doi.org/10.3390/safety12030059.
44. Cvetković, V.M.; Milenković, D.; Lukić, T.; Renner, R. Theoretical evolution of measuring community resilience to natural and technological disasters: Past, present, and future—Empirical insights from qualitative research in Serbia. *Open Geosci.* **2026**, *18*, 20250968. https://doi.org/10.1515/geo-2025-0968.
45. Nikolić, N.; Cvetković, V.M.; Renner, R.; Cvijović, N.; Gačić, J. Disaster risk perception and local resilience near the "Duboko" landfill: Challenges of governance, management, trust, and environmental communication in Serbia. *Open Geosci.* **2025**, *17*, 20250850. https://doi.org/10.1515/geo-2025-0850.
46. Cvetković, V.; Roder, G.; Öcal, A.; Tarolli, P.; Dragićević, S. The role of gender in preparedness and response behaviors towards flood risk in Serbia. *Int. J. Environ. Res. Public Health* **2018**, *15*, 2761. https://doi.org/10.3390/ijerph15122761.
47. Cvetković, V.; Ronan, K.; Shaw, R.; Filipović, M.; Mano, R.; Gačić, J.; Jakovljević, V. Household earthquake preparedness in Serbia: A study of selected municipalities. *Acta Geogr. Slov.* **2019**, *59*, 27–42. https://doi.org/10.3986/AGS.5445.
48. Trgovčević, F.; Stupar, A.; Ivanović, M.; Susman, R. Toward flood resilience in Serbia: The challenges of an (un)sustainable policy. *Sustainability* **2020**, *12*, 7228. https://doi.org/10.3390/su12177228.
49. Beli, A.; Renner, R.; Cvetković, V.M.; Ivanov, A.; Gačić, J. A cross-national study of disaster risk management: Strengths and weaknesses in Bulgaria, Romania, and Albania with reflections on Serbia. *Int. J. Disaster Risk Manag.* **2025**, *7*, 431–460. https://doi.org/10.18485/ijdrm.2025.7.1.25.
50. Beccari, B. A comparative analysis of disaster risk, vulnerability and resilience composite indicators. *PLoS Curr.* **2016**, *8*. https://doi.org/10.1371/currents.dis.453df025e34b682e9737f95070f9b970.
51. Marzi, S.; Mysiak, J.; Essenfelder, A.; Amadio, M.; Giove, S.; Fekete, A. Constructing a comprehensive disaster resilience index: The case of Italy. *PLoS ONE* **2019**, *14*, e0221585. https://doi.org/10.1371/journal.pone.0221585.

52. Sibilia, A.; Eklund, G.; Marzi, S.; Valli, I.; Bountzouklis, C.; Roeslin, S.; Rodomonti, D.; Salari, S.; Antofie, T.-E.; Corbane, C. Developing a multi-level European-wide composite indicator to assess vulnerability dynamics across time and space. *Int. J. Disaster Risk Reduct.* **2024**, *113*, 104885. https://doi.org/10.1016/j.ijdrr.2024.104885.
53. Painter, M.A.; Shah, S.H.; Damestoit, G.C.; Khalid, F.; Prudencio, W.; Chisty, M.A.; Tormos-Aponte, F.; Wilhelmi, O. A systematic scoping review of the Social Vulnerability Index as applied to natural hazards. *Nat. Hazards* **2024**, *120*, 7265–7356. https://doi.org/10.1007/s11069-023-06378-z.
54. Mah, J.C.; Penwarden, J.L.; Pott, H.; Theou, O.; Andrew, M.K. Social vulnerability indices: A scoping review. *BMC Public Health* **2023**, *23*, 1253. https://doi.org/10.1186/s12889-023-16097-6.
55. Raduszynski, T.; Numada, M. Measure and spatial identification of social vulnerability, exposure and risk to natural hazards in Japan using open data. *Sci. Rep.* **2023**, *13*, 664. https://doi.org/10.1038/s41598-023-27831-w.
56. Chelariu, O.E.; Minea, I.; Iatu, C. Integrated assessment of geophysical and social vulnerability to natural hazards in North-East Region, Romania. *Geomat. Nat. Hazards Risk* **2024**, *15*, 2384607. https://doi.org/10.1080/19475705.2024.2384607.
57. Galderisi, A.; Limongi, G. A comprehensive assessment of exposure and vulnerabilities in multi-hazard urban environments: A key tool for risk-informed planning strategies. *Sustainability* **2021**, *13*, 9055. https://doi.org/10.3390/su13169055.
58. Tascón-González, L.; Ferrer-Juliá, M.; Ruiz, M.; García-Meléndez, E. Social vulnerability assessment for flood risk analysis. *Water* **2020**, *12*, 558. https://doi.org/10.3390/w12020558.
59. Zhou, S.; Zhai, G. A multi-hazard risk assessment framework for urban disaster prevention planning: A case study of Xiamen, China. *Land* **2023**, *12*, 1884. https://doi.org/10.3390/land12101884.
60. Derakhshan, S.; Emrich, C.; Cutter, S. Degree and direction of overlap between social vulnerability and community resilience measurements. *PLoS ONE* **2022**, *17*, e0275975. https://doi.org/10.1371/journal.pone.0275975.
61. Norris, F.H.; Stevens, S.P.; Pfefferbaum, B.; Wyche, K.F.; Pfefferbaum, R.L. Community resilience as a metaphor, theory, set of capacities, and strategy for disaster readiness. *Am. J. Community Psychol.* **2008**, *41*, 127–150. https://doi.org/10.1007/s10464-007-9156-6.
62. Sherrieb, K.; Norris, F.H.; Galea, S. Measuring capacities for community resilience. *Soc. Indic. Res.* **2010**, *99*, 227–247. https://doi.org/10.1007/s11205-010-9576-9.
63. Pfefferbaum, B.; Pfefferbaum, R.L.; Van Horn, R.L. Community resilience interventions: Participatory, assessment-based, action-oriented processes. *Am. Behav. Sci.* **2015**, *59*, 238–253. https://doi.org/10.1177/0002764214550298.
64. Pfefferbaum, B.; Van Horn, R.L.; Pfefferbaum, R.L. A conceptual framework to enhance community resilience using social capital. *Clin. Soc. Work J.* **2017**, *45*, 102–110. https://doi.org/10.1007/s10615-015-0556-z.
65. Orencio, P.M.; Fujii, M. A localized disaster-resilience index to assess coastal communities based on an analytic hierarchy process (AHP). *Int. J. Disaster Risk Reduct.* **2013**, *3*, 62–75. https://doi.org/10.1016/j.ijdrr.2012.11.006.
66. Mavhura, E.; Manyangadze, T.; Aryal, K. A composite inherent resilience index for Zimbabwe: An adaptation of the Disaster Resilience of Place model. *Int. J. Disaster Risk Reduct.* **2021**, *57*, 102152. https://doi.org/10.1016/j.ijdrr.2021.102152.
67. Azzimonti, O.; Colleoni, M.; De Amicis, M.; Frigerio, I. Combining hazard, social vulnerability and resilience to provide a proposal for seismic risk assessment. *J. Risk Res.* **2020**, *23*, 1225–1241. https://doi.org/10.1080/13669877.2019.1646308.
68. Bakhtiari, S.; Najafi, M.R.; Goda, K.; Peerhossaini, H. A dynamic Bayesian network approach to characterize multi-hazard risks and resilience in interconnected critical infrastructures. *Reliab. Eng. Syst. Saf.* **2025**, *257*, 110815. https://doi.org/10.1016/j.ress.2025.110815.
69. Triyanti, A.; Surtiari, G.A.K.; Lassa, J.A.; Rafliana, I.; Hanifa, N.R.; Muhidin, M.I.; Djalante, R. Governing systemic and cascading disaster risk in Indonesia: Where do we stand and future outlook. *Disaster Prev. Manag.* **2023**, *32*, 27–48. https://doi.org/10.1108/DPM-07-2022-0156.
70. Schlumberger, J.; Haasnoot, M.; Aerts, J.; de Ruiter, M.D. Proposing DAPP-MR as a disaster risk management pathways framework for complex, dynamic multi-risk. *iScience* **2022**, *25*, 105219. https://doi.org/10.1016/j.isci.2022.105219.
71. Delves, J.L.; Renner, K.; Campalani, P.; Piñon, J.; Schneiderbauer, S.; Moreno, M.; Oterino, M.B.B.; Perez, E.; Pittore, M. Comprehensive multi-hazard risk assessment in data-scarce regions: A study focused on Burundi. *Nat. Hazards Earth Syst. Sci.* **2026**, *26*, 1347–1373. https://doi.org/10.5194/nhess-26-1347-2026.
72. Canete, R.; Biñas, R. Differential risk and the elements of resilience: A framework for advancing disaster risk reduction. *Int. J. Disaster Risk Manag.* **2025**, *7*, 209–238. https://doi.org/10.18485/ijdrm.2025.7.2.12.
73. Pradhan, B.; Kumar, S.; Nayak, D. From vulnerability to resilience: A systematic review of Odisha's integrated approach to disaster risk reduction. *Int. J. Disaster Risk Manag.* **2025**, *7*, 519–532. https://doi.org/10.18485/ijdrm.2025.7.1.30.

74. Koech, H. Recurrent urban flooding in Nairobi City: A systematic review of environmental determinants, public health impacts and policy gaps. *Int. J. Disaster Risk Manag.* **2026**, *8*, 331–366. https://doi.org/10.66050/ac1fpr38.
75. Krausmann, E.; Cozzani, V.; Salzano, E.; Renni, E. Industrial accidents triggered by natural hazards: An emerging risk issue. *Nat. Hazards Earth Syst. Sci.* **2011**, *11*, 921–929. https://doi.org/10.5194/nhess-11-921-2011.
76. Laurien, F.; Martin, J.G.C.; Mehryar, S. Climate and disaster resilience measurement: Persistent gaps in multiple hazards, methods, and practicability. *Clim. Risk Manag.* **2022**, *37*, 100443. https://doi.org/10.1016/j.crm.2022.100443.
77. Bucherie, A.; Hultquist, C.; Adamo, S.B.; Neely, C.; Ayala, F.; Bazo, J.; Kruczkiewicz, A. A comparison of social vulnerability indices specific to flooding in Ecuador: Principal component analysis and expert knowledge. *Int. J. Disaster Risk Reduct.* **2022**, *73*, 102897. https://doi.org/10.1016/j.ijdrr.2022.102897.
78. Sabljić, L.; Lukić, T.; Bajić, D.; Marković, S.B.; Spalevic, V.; Cvetković, V.; Delić, D.; Adžić, D.; Aleksova, B.; Milevski, I.; et al. Spatio-temporal analysis of flood events using GIS and remote sensing-based approach in the Ukrina River Basin, Bosnia and Herzegovina. *Open Geosci.* **2025**, *17*, 20250856. https://doi.org/10.1515/geo-2025-0856.
79. Sabljić, L.; Bajić, D.; Marković, S.B.; Adžić, D.; Spalevic, V.; Sestraș, P.; Pavić, D.; Lukić, T. Remote sensing and GIS assessment of drought dynamics in the Ukrina River Basin, Bosnia and Herzegovina. *Atmosphere* **2026**, *17*, 124. https://doi.org/10.3390/atmos17020124.
80. Nelson, C.D.; Lurie, N.; Wasserman, J.; Zakowski, S. Conceptualizing and defining public health emergency preparedness. *Am. J. Public Health* **2007**, *97*, S9–S11. https://doi.org/10.2105/AJPH.2007.114496.
81. Savoia, E.; Testa, M.A.; Biddinger, P.D.; Cadigan, R.O.; Koh, H.; Campbell, P.; Stoto, M.A. Assessing public health capabilities during emergency preparedness tabletop exercises: Reliability and validity of a measurement tool. *Public Health Rep.* **2009**, *124*, 138–148. https://doi.org/10.1177/003335490912400117.
82. Khan, Y.; Brown, A.D.; Gagliardi, A.; O'Sullivan, T.; Lacarte, S.; Henry, B.; Schwartz, B. Are we prepared? The development of performance indicators for public health emergency preparedness using a modified Delphi approach. *PLoS ONE* **2019**, *14*, e0226489. https://doi.org/10.1371/journal.pone.0226489.
83. Sasie, S.D.; Ayano, G.; Van Zuylen, P.; Aragaw, F.M.; Darebo, T.D.; Guerrero-Torres, L.; Mulugeta, A.; Spigt, M. Developing a comprehensive framework for evaluating public health emergency management program implementation: A scoping review. *Public Health* **2025**, *239*, 22–31. https://doi.org/10.1016/j.puhe.2024.12.012.
84. Wen, Q.; Ismail, M.; Abdul Nasir, M.H. A community public health emergency resilience assessment framework based on contrastive learning and hyperbolic embedding. *Front. Public Health* **2025**, *13*, 1651331. https://doi.org/10.3389/fpubh.2025.1651331.
85. Hunter, J.; Yang, J.E.; Petrie, M.C.; Aragón, T. Integrating a framework for conducting public health systems research into statewide operations-based exercises to improve emergency preparedness. *BMC Public Health* **2012**, *12*, 680. https://doi.org/10.1186/1471-2458-12-680.
86. Goode, E.-J.; Thomas, E.; Landeg, O.; Duarte-Davidson, R.; Hall, L.; Roelofs, J.; Schulpen, S.; De Bruin, A.; Wigenstam, E.; Liljedahl, B.; et al. Development of a rapid risk and impact assessment tool to enhance response to environmental emergencies in the early stages of a disaster: A Tool Developed by the European Multiple Environmental Threats Emergency NETwork (EMETNET) Project. *Int. J. Disaster Risk Sci.* **2021**, *12*, 528–539. https://doi.org/10.1007/s13753-021-00352-8.
87. World Health Organization. *International Health Regulations (2005)*, 3rd ed.; WHO: Geneva, Switzerland, 2016. Available online: https://www.who.int/publications/i/item/9789241580496 (accessed on 18 January 2026).
88. World Health Organization. *Communicating Risk in Public Health Emergencies: A WHO Guideline for Emergency Risk Communication (ERC) Policy and Practice*; WHO: Geneva, Switzerland, 2017. Available online: https://www.who.int/publications/i/item/9789241550208 (accessed on 28 March 2026).
89. World Health Organization. *Health Emergency and Disaster Risk Management Framework*; WHO: Geneva, Switzerland, 2019. Available online: https://www.who.int/publications/i/item/9789241516181 (accessed on 28 March 2026).
90. World Health Organization. *2019 Novel Coronavirus (2019-nCoV): Strategic Preparedness and Response Plan*; WHO: Geneva, Switzerland, 2020. Available online: https://www.who.int/publications/i/item/strategic-preparedness-and-response-plan-for-the-new-coronavirus (accessed on 15 June 2026).
91. Djebari, S.; Bestandji, S. The role of spatial analysis in notifiable disease monitoring and health risk management: A case study of Constantine. *Int. J. Disaster Risk Manag.* **2025**, *7*, 215–233. https://doi.org/10.18485/ijdrm.2025.7.1.12.
92. Ivanov, A. Disaster risk reduction and disaster risk management: State of play in North Macedonia. *Int. J. Disaster Risk Manag.* **2024**, *6*, 201–212. https://doi.org/10.18485/ijdrm.2024.6.2.13.

93. Kapucu, N. Collaborative emergency management: Better community organising, better public preparedness and response. *Disasters* **2008**, *32*, 239–262. https://doi.org/10.1111/j.1467-7717.2008.01037.x.
94. Tiernan, A.; Drennan, L.; Nalau, J.; Onyango, E.; Morrissey, L.; Mackey, B. A review of themes in disaster resilience literature and international practice since 2012. *Policy Des. Pract.* **2019**, *2*, 53–74. https://doi.org/10.1080/25741292.2018.1507240.
95. Räsänen, A.; Lein, H.; Bird, D.; Setten, G. Conceptualizing community in disaster risk management. *Int. J. Disaster Risk Reduct.* **2020**, *45*, 101485. https://doi.org/10.1016/j.ijdrr.2020.101485.
96. Ryan, B.; Johnston, K.A.; Taylor, M.; McAndrew, R. Community engagement for disaster preparedness: A systematic literature review. *Int. J. Disaster Risk Reduct.* **2020**, *49*, 101655. https://doi.org/10.1016/j.ijdrr.2020.101655.
97. Vandrevala, T.; Morrow, E.; Coates, T.; Boulton, R.; Crawshaw, A.; O'Dwyer, E.; Heitmeyer, C. Strengthening the relationship between community resilience and health emergency communication: A systematic review. *BMC Glob. Public Health* **2024**, *2*, 79. https://doi.org/10.1186/s44263-024-00112-y.
98. Hinata, S.; Rohde, H.; Templeton, A. Communicating with the public in emergencies: A systematic review of communication approaches in emergency response. *Int. J. Disaster Risk Reduct.* **2024**, *111*, 104719. https://doi.org/10.1016/j.ijdrr.2024.104719.
99. Sufri, S.; Dwirahmadi, F.; Phung, D.; Rutherford, S. A systematic review of community engagement in disaster early warning systems. *Prog. Disaster Sci.* **2020**, *5*, 100058. https://doi.org/10.1016/j.pdisas.2019.100058.
100. Jha, A.; Lin, L.; Short, S.M.; Argentini, G.; Gamhewage, G.; Savoia, E. Integrating emergency risk communication into the public health system response: Systematic review of literature to aid formulation of the 2017 WHO guideline for ERC policy and practice. *PLoS ONE* **2018**, *13*, e0205555. https://doi.org/10.1371/journal.pone.0205555.
101. Toppenberg-Pejcic, D.; Noyes, J.; Allen, T.; Alexander, N.; Vanderford, M.L.; Gamhewage, G. Emergency risk communication: Lessons learned from a rapid review of recent gray literature on Ebola, Zika, and yellow fever. *Health Commun.* **2019**, *34*, 437–455. https://doi.org/10.1080/10410236.2017.1405488.
102. Novak, J.; Day, A.; Sopory, P.; Wilkins, L.; Padgett, D.; Eckert, S.; Noyes, J.; Allen, T.; Alexander, N.; Vanderford, M.; et al. Engaging communities in emergency risk and crisis communication: A systematic review and evidence synthesis. *J. Int. Crisis Risk Commun. Res.* **2019**, *2*, 61–96. https://doi.org/10.30658/jicrcr.2.1.4.
103. Khan, S.; Mishra, J.; Ahmed, N.; Onyige, C.D.; Lin, K.E.; Siew, R.; Lim, B.H. Risk communication and community engagement during COVID-19. *Int. J. Disaster Risk Reduct.* **2022**, *74*, 102903. https://doi.org/10.1016/j.ijdrr.2022.102903.
104. Tambo, E.; Djuikoue, I.C.; Tazemda, G.K.; Fotsing, M.F.; Zhou, X.-N. Early stage risk communication and community engagement (RCCE) strategies and measures against the coronavirus disease 2019 (COVID-19) pandemic crisis. *Glob. Health J.* **2021**, *5*, 44–50. https://doi.org/10.1016/j.glohj.2021.02.009.
105. Stewart, I. Advancing disaster risk communications. *Earth-Sci. Rev.* **2024**, *249*, 104677. https://doi.org/10.1016/j.earscirev.2024.104677.
106. Fathollahzadeh, A.; Salmani, I.; Morowatisharifabad, M.; Khajehaminian, M.; Babaie, J.; Fallahzadeh, H. Models and components in disaster risk communication: A systematic literature review. *J. Educ. Health Promot.* **2023**, *12*, 87. https://doi.org/10.4103/jehp.jehp_277_22.
107. Agyepong, L.A.; Liang, X. Mapping the knowledge frontiers of public risk communication in disaster risk management. *J. Risk Res.* **2023**, *26*, 302–323. https://doi.org/10.1080/13669877.2022.2127851.
108. Bonfanti, R.C.; Oberti, B.; Ravazzoli, E.; Rinaldi, A.; Ruggieri, S.; Schimmenti, A. The role of trust in disaster risk reduction: A critical review. *Int. J. Environ. Res. Public Health* **2024**, *21*, 29. https://doi.org/10.3390/ijerph21010029.
109. Nicholas, J.P.; Donovan, A.; Oppenheimer, C.; Bell, L.; Van Wyk de Vries, M. How trust shapes individual resilience to natural hazards: A systematic review. *Nat. Hazards* **2026**, *122*, 48. https://doi.org/10.1007/s11069-025-07816-w.
110. Wisner, B.; Blaikie, P.; Cannon, T.; Davis, I. *At Risk: Natural Hazards, People's Vulnerability and Disasters*, 2nd ed.; Routledge: London, UK, 2004.
111. Tierney, K.J. *The Social Roots of Risk: Producing Disasters, Promoting Resilience*; Stanford University Press: Stanford, CA, USA, 2014.
112. Slovic, P. Perception of risk. *Science* **1987**, *236*, 280–285. https://doi.org/10.1126/science.3563507.
113. Douglas, M.; Wildavsky, A. *Risk and Culture: An Essay on the Selection of Technological and Environmental Dangers*; University of California Press: Berkeley, CA, USA, 1982.
114. Funtowicz, S.O.; Ravetz, J.R. Science for the post-normal age. *Futures* **1993**, *25*, 739–755. https://doi.org/10.1016/0016-3287(93)90022-L.
115. Unaam, A. Institutionalizing disaster risk reduction in fragile states: Local governance capacity, conflict insecurity, and community resilience in Lower Juba, Somalia. *Int. J. Disaster Risk Manag.* **2026**, *8*, 367–384. https://doi.org/10.66050/c06z9913.

116. Uddin, M.S.; Haque, C.E.; Khan, M.N. Good governance and local level policy implementation for disaster-risk-reduction: Actual, perceptual and contested perspectives in coastal communities in Bangladesh. *Disaster Prev. Manag.* **2021**, *30*, 94–111. https://doi.org/10.1108/DPM-03-2020-0069.
117. Sukhwani, V.; Gyamfi, B.A.; Zhang, R.; AlHinai, A.M.; Shaw, R. Understanding the barriers restraining effective operation of flood early warning systems. *Int. J. Disaster Risk Manag.* **2019**, *1*, 1–17. https://doi.org/10.18485/ijdrm.2019.1.2.1.
118. Rico, G.C.S. School-community collaboration: Disaster preparedness towards building resilient communities. *Int. J. Disaster Risk Manag.* **2019**, *1*, 45–61. https://doi.org/10.18485/ijdrm.2019.1.2.4.
119. Sacyaten, C.S. Crisis communication in times of disasters: Public perceptions on the timeliness and clarity of safety announcements: A systematic literature review. *Int. J. Disaster Risk Manag.* **2025**, *7*, 193–208. https://doi.org/10.18485/ijdrm.2025.7.2.11.
120. Yamah, D.; Folorunsho, T. Leveraging social media and mobile technology for disaster communication in Nigeria. *Int. J. Disaster Risk Manag.* **2026**, *8*, 1–30. https://doi.org/10.66050/x77jr639.
121. Latvakoski, J.; Öörni, R.; Lusikka, T.; Keränen, J. Evaluation of emerging technological opportunities for improving risk awareness and resilience of vulnerable people in disasters. *Int. J. Disaster Risk Reduct.* **2022**, *80*, 103173. https://doi.org/10.1016/j.ijdrr.2022.103173.
122. Cutter, S.L.; Barnes, L.; Berry, M.; Burton, C.; Evans, E.; Tate, E.; Webb, J. A place-based model for understanding community resilience to natural disasters. *Glob. Environ. Change* **2008**, *18*, 598–606. https://doi.org/10.1016/j.gloenvcha.2008.07.013.
123. Cutter, S.L.; Ash, K.D.; Emrich, C.T. The geographies of community disaster resilience. *Glob. Environ. Change* **2014**, *29*, 65–77. https://doi.org/10.1016/j.gloenvcha.2014.08.005.
124. Stough, L.M.; Kang, D. The Sendai Framework for Disaster Risk Reduction and Persons with Disabilities. *Int. J. Disaster Risk Sci.* **2015**, *6*, 140–149. https://doi.org/10.1007/s13753-015-0051-8.
125. Ouyang, M. Review on modeling and simulation of interdependent critical infrastructure systems. *Reliab. Eng. Syst. Saf.* **2014**, *121*, 43–60. https://doi.org/10.1016/j.ress.2013.06.040.

Disclaimer/Publisher's Note: The statements, opinions and data contained in all publications are solely those of the individual author(s) and contributor(s) and not of MDPI and/or the editor(s). MDPI and/or the editor(s) disclaim responsibility for any injury to people or property resulting from any ideas, methods, instructions or products referred to in the content.